Elementa: Science of the Anthropocene

Meteorological conditions during the MOSAiC expedition: Normal or anomalous?

--Manuscript Draft--

Manuscript Number:	ELEMENTA-D-21-00023R1
Full Title:	Meteorological conditions during the MOSAiC expedition: Normal or anomalous?
Short Title:	MOSAiC meteorological conditions
Article Type:	Research Article
Section/Category:	Atmospheric Science Domain
Manuscript Classifications:	Atmospheric Science
Abstract:	This paper sets the near-surface meteorological conditions during the Multidisciplinary drifting Observatory for the Study of Arctic Climate (MOSAiC) expedition in the context of the interannual variability and extremes within the past four decades. Hourly ERA5 reanalysis data for the Polarstern trajectory for 1979-2020 are analyzed. The conditions were relatively normal given that they were mostly within the interquartile range of the preceding four decades. Nevertheless, some anomalous and even record-breaking conditions did occur, particularly during synoptic events. Extreme cases of warm, moist air transported from the northern North Atlantic or northwestern Siberia into the Arctic were identified from late fall until early spring. Daily temperature and total column water vapor were classified as being among the top-ranking warmest/wettest days or even record-breaking based on the full record. Associated with this, the longwave radiative fluxes at the surface were extremely anomalous for these winter cases. The winter and spring period was characterized by more frequent storm events and median cyclone intensity ranking in the top 25th percentile of the full record. During summer, near melting point conditions were more than a month longer than usual and the July and August 2020 mean conditions were the all-time warmest and wettest. These record conditions near the Polarstern were embedded in large positive temperature and moisture anomalies over the whole central Arctic. In contrast, unusually cold conditions occurred during the beginning of November 2019 and in early March 2020, related to the Arctic Oscillation. In March, this was linked with anomalously strong and persistent northerly winds associated with frequent cyclone occurrence to the southeast of the Polarstern.
Corresponding Author:	John Cassano UNITED STATES
Corresponding Author E-Mail:	john.cassano@Colorado.EDU
Other Authors:	Annette Rinke
	Elizabeth Cassano
	Ralf Jaiser
	Dörthe Handorf
Order of Authors:	Annette Rinke
	John Cassano
	Elizabeth Cassano
	Ralf Jaiser
	Dörthe Handorf
Order of Authors Secondary Information:	
First Author:	Annette Rinke
Manuscript Region of Origin:	UNITED STATES
Suggested Reviewers:	Timo Vihma Finnish Meteorological Institute: Ilmatieteen Laitos

	Timo.Vihma@fmi.fi Expert in that field
	Michael Tjernström Stockholm University: Stockholms Universitet michaelt@misu.su.se Expert in that field
	Julia Schmale ETH Zurich D-USYS: Eidgenossische Technische Zurich Hochschule Departement Umweltsystemwissenschaften julia.schmale@epfl.ch Expert in that fields
	Malte Mueller Norwegian Meteorological Institute: Meteorologisk institutt maltem@met.no Expert in that field
	Matts Granskog Norwegian Polar Institute: Norsk Polarinstitutt mats.granskog@npolar.no
Opposed Reviewers:	
Response to Reviewers:	Please see the attached response to all reviewer and editor comments.
Additional Information:	
Question	**Response**
Is your submission a part of a Special Feature?	Yes
Please provide the Special Feature title. as follow-up to "**Is your submission a part of a Special Feature?**"	The Multidisciplinary Drifting Observatory for the Study of Arctic Climate (MOSAiC)
Is your submission a part of a Forum?	No
How did you first hear about Elementa? Please choose from the list below or describe other if applicable.	At a conference
What were your main motivations to publish with Elementa? Please select all that apply.	My manuscript is part of a Special Feature; Desire to publish in an open access publication; Elementa's multidisciplinary scope; Colleague recommendation
Publication Charges The costs of producing and maintaining *Elementa* are recovered by charging a publication fee to authors or research sponsors for each article accepted for publication. Currently the publication fee is $1,450 for all article types except Commentary and Comment and Reply, which are $650. A portion of every APC collected from authors (currently, $250 per article) is automatically allocated to a	Authors have funds to cover APC

fee waiver fund that is used to help authors who lack external or institutional funding pay their publication fees.

UC Press has partnered with Copyright Clearance Center (CCC) to process author APC payments. Upon acceptance of a paper for publication the corresponding author will receive an email with detailed instructions and a link to either pay the fee through CCC's secure e-commerce system or generate an invoice, which can be used to pay by check, wire, or other means. **Accepted articles will not be published until funds have been received.**

Because we try to keep our APCs low, and because a portion of the proceeds is diverted to a waiver fund, we ask that all of those who have the means to pay refrain from requesting fee waivers and other discounts. Your payments ensure that as many researchers as possible have the opportunity to publish in the journal.

Authors who lack the funds to cover publication fees may request a waiver. In order to keep publication charges as low as possible, fee waivers are not automatically given but must be approved on a case-by-case basis.

APC Discounts and Waivers
The University of California Press offers several discount and waiver programs in order to try to ensure that anyone wishing to publish in the journal has the opportunity to do so without regard to their ability to pay. In some cases, the discount may be applied automatically, and in other cases, it must be requested.

University of California fee waiver—Fees are currently waived for all faculty, staff, and students of the University of California system. The Editorial Committee of the Academic Senate has

allocated funding specifically for this use. The waiver will be applied upon acceptance of the article. **Discount for authors from low and middle-income countries**—Corresponding authors whose primary affiliations are eligible for the Research4Life program, Groups A & B, are currently automatically offered a 75% discount through CCC's e-commerce system. This discount will be applied when an eligible author clicks the link to pay their fees or generate an invoice for payment. **Full Fee Waivers**— If you are unable to pay the APC for your article, you may request a fee waiver below. A member of the UC Press team will be in contact with you regarding your waiver request as soon as it is received. Waiver requests are subject to the availability of funding in the fee waiver fund. Please select the appropriate answer below. The corresponding author answers the question below on behalf of all manuscript authors.	
Author Comments:	

National Snow and Ice Data Center
University of Colorado Boulder
nsidc.org

John J. Cassano
Fellow, Cooperative Institute for Research in Environmental Sciences
Lead Scientist, National Snow and Ice Data Center
Professor, Department of Atmospheric and Oceanic Sciences
University of Colorado – Boulder

31 May 2021

Dear Dr. Helmig,

Please find enclosed the revisions to our manuscript “Meteorological Conditions During the MOSAiC Expedition: Normal or Anomalous?”. We have addressed all of the reviewer concerns and include a clean version of the revised manuscript, a revised manuscript with tracked changes, our response to all reviewer comments, a file containing all figures and a file with our supplementary material.

Please let me know if you need any additional items to continue the review process for this manuscript.

Best regards,

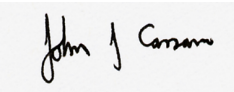

John J. Cassano

449 UCB
University of Colorado
Boulder, CO 80309-0449
Phone: +1 303 492 6199
Fax: +1 303 492 2486
Email: nsidc@nsidc.org

Meteorological conditions during the MOSAiC expedition: Normal or anomalous?

Annette Rinke[1)#], John Cassano[2, 3)#*], Elizabeth Cassano[2)], Ralf Jaiser[1)], Dörthe Handorf[1)]

[1)] Alfred Wegener Institute, Helmholtz Centre for Polar and Marie Research (AWI), Potsdam, Germany
[2)] National Snow and Ice Data Center, Cooperative Institute for Research in Environmental Sciences (CIRES), University of Colorado, Boulder, CO, USA
[3)] Department of Atmospheric and Oceanic Sciences, University of Colorado, Boulder, CO USA

[#] These authors contributed equally to this work.

[*] Corresponding author: John Cassano (john.cassano@Colorado.EDU)

Abstract. This paper sets the near-surface meteorological conditions during the Multidisciplinary drifting Observatory for the Study of Arctic Climate (MOSAiC) expedition in the context of the interannual variability and extremes within the past four decades. Hourly ERA5 reanalysis data for the *Polarstern* trajectory for 1979-2020 are analyzed. The conditions were relatively normal given that they were mostly within the interquartile range of the preceding four decades. Nevertheless, some anomalous and even record-breaking conditions did occur, particularly during synoptic events. Extreme cases of warm, moist air transported from the northern North Atlantic or northwestern Siberia into the Arctic were identified from late fall until early spring. Daily temperature and total column water vapor were classified as being among the top-ranking warmest/wettest days or even record-breaking based on the full record. Associated with this, the longwave radiative fluxes at the surface were extremely anomalous for these winter cases. The winter and spring period was characterized by more frequent storm events and median cyclone intensity ranking in the top 25th percentile of the full record. During summer, near melting point conditions were more than a month longer than usual and the July and August 2020 mean conditions were the all-time warmest and wettest. These record conditions near the *Polarstern* were embedded in large positive temperature and moisture anomalies over the whole central Arctic. In contrast, unusually cold conditions occurred during the beginning of November 2019 and in early March 2020, related to the Arctic Oscillation. In March, this was linked with anomalously strong and persistent northerly winds associated with frequent cyclone occurrence to the southeast of the *Polarstern*.

1. Introduction

The Multidisciplinary drifting Observatory for the Study of Arctic Climate (MOSAiC) expedition (Shupe et al., 2020) was a yearlong (October 2019-September 2020) drift with the sea ice across the central Arctic Ocean, based around the German icebreaker *Polarstern*. Its overarching goal was to study the climate of the "new" Arctic (https://mosaic-expedition.org/wp-content/uploads/2020/12/mosaic_scienceplan.pdf), which is characterized by warming temperatures, retreating and thinning sea ice, and changing atmospheric and ocean circulation (e.g., Stroeve and Notz, 2018; Box et al., 2019). A major goal of MOSAiC is to improve the understanding of Arctic climate processes and the complex interactions and feedbacks within the coupled atmosphere-ice-ocean-biogeochemistry-ecosystem. To place the single MOSAiC year of data in a broader climate context it is important to know if the expedition occurred under 'normal' or 'unusual' conditions. This study focusses on the near-surface meteorological conditions experienced during the MOSAiC expedition and compares these to a long-term reanalysis record.

Before the start of MOSAiC, the conditions in the Arctic were exceptional with record warm air temperatures in summer 2019, the longest ice-free summer period since 1979, and unusually thin sea ice (Krumpen et al., 2020). The MOSAiC winter of 2019/2020 attracted a lot of attention, because the Arctic stratosphere featured an exceptionally strong and cold polar vortex and related extreme ozone loss, accompanied by an unprecedentedly positive phase of the Arctic Oscillation (AO) during January-March 2020 (Wohltmann et al., 2020; Lawrence et al., 2020; Manney et al., 2020). Related to this, unprecedented warming over Eurasia and particularly the Kara and Laptev Seas regions was reported for those winter months. During spring and summer 2020 mean temperatures were above normal for most of the Arctic (Ballinger et al., 2020), with Siberia observing record-breaking temperatures associated with a persistent Siberian heatwave (Overland and Wang, 2020). For the actual MOSAiC drift path and speed, and the sea-ice conditions (such as thickness, melt ponds etc.), the atmospheric circulation patterns and associated anomalies in near-surface wind, temperature and radiation are relevant.

The aim of this paper is to characterize the 12-month time series of near-surface meteorological conditions during the MOSAiC expedition and compare this with the previous 41 years (1979-2019). This study is based on the European Centre for Medium-range Weather Forecasts (ECMWF) reanalysis ERA5 (Hersbach et al., 2020). This reanalysis has been selected because of its high resolution (ca. 30 km horizontal and 1 hourly temporal resolutions) and use of a significantly more advanced 4D-var assimilation scheme, as well as its improved performance over the Arctic (Graham et al., 2019a, b). Still, similar to other reanalyses, ERA5 struggles with a few Arctic specifics. These include a positive wintertime 2 m air temperature bias which is largest during very cold stable conditions and is associated with poorly represented surface inversions and turbulent heat fluxes over sea ice (Graham et al., 2019b). However, since these are systematic biases, and because this study compares ERA5 conditions during the MOSAiC year to ERA5 conditions during the previous four decades these biases are likely not relevant. Future work, based on MOSAiC meteorological observations can provide a comparison between ERA5 and the actual meteorology observed during the expedition, but since these data are currently still being quality controlled, the current reanalysis-only results presented here provides a first assessment of the MOSAiC expedition meteorology and its comparison to the prior decades.

By assessing the MOSAiC's meteorological conditions in the context of interannual variability and extremes within the past four decades, this study will document if the MOSAiC conditions, along the drift track, were close to the long-term mean or exceptional and identify any record conditions. Furthermore, this analysis will highlight some interesting meteorological situations and synoptic events that can be the focus of future studies.

2. Data based on ERA5

Statistics of near-surface meteorological conditions and cyclones, based on ERA5, are calculated for each month of the MOSAiC year, from October 2019 to September 2020, as well as for the previous 41 years from 1979 to 2019. The latter period is used as the long-term reference. The statistics for the MOSAiC and pre-MOSAiC years are compared. For the latter, the median, interquartile range (25^{th}-75^{th} percentiles, IQR), 5^{th} and 95^{th} percentiles, and minimum and maximum of the variables are calculated based on 1979-2019. This does not include the MOSAiC year and is so based on the period from 1 January 1979 to 30 September 2019. It is important to note that ERA5 assimilates the *Polarstern* sounding and the weather station data that is distributed on the GTS.

To characterize the MOSAiC data with respect to the previous four decades, we apply the following description. If the data are within the IQR we consider them being 'normal'. If the data are out of IQR but still within the 5^{th}-95^{th} percentile range we consider them 'unusual' or 'anomalous'. If data are above/below the 95^{th}/5^{th} percentiles we consider them being 'extremely anomalous' or 'record-breaking'. This is equivalent with the three top highest/lowest rankings considering the full record 1979-2020. The application of a standard 30-year climatological reference period from 1981-2010 confirms our conclusions about the 'anomalous' events. In addition, we used the recent decade 2010-2019 as a reference period to characterize the state of the 'new Arctic'.

We cover the full annual cycle of MOSAiC. This includes the passive (drifting) and active (steaming) ship time. At the following dates the *Polarstern* was located at a permanent ice station and passively drifting with the ice: 4 October 2019 - 15 May 2020 (Legs 1-3), 18 June 2020 - 30 July 2020 (Leg 4), and 22 August 2020 - 19 September 2020 (Leg 5).

2.1 Near-surface meteorological data

The following ERA5 data were used to characterize the near-surface meteorological conditions: mean sea level pressure (MSLP), 2 m and 850 hPa air temperature, 10 m wind speed and direction, total column water vapor (TCWV), and surface radiation components. For these variables, hourly ERA5 data from 1 October 2019 through 30 September 2020 (Figure S1) were extracted for the four grid points nearest the *Polarstern* position. Along the same MOSAiC trajectory the hourly four-grid-points data were extracted for the preceding 41 years of 1979-2019. In addition to the time series, box plots (with median, IQR, minimum-maximum range) and the Probability Density Functions (PDFs) from Kernel density estimation with Gaussian kernels are presented to identify changes in the distribution of the considered variables. To identify any record conditions, we ranked both the daily and monthly values for the full period from 1979-2020. All results are the same regardless if one simply averages the four grid points or calculates a distance-weighted average, thus the first approach is used. Spatial monthly anomaly maps with respect to the 41-year climatology are calculated to indicate regionally unusual conditions.

2.2 Cyclone detection and tracking

Along with the near-surface meteorological conditions described above, cyclones that impacted the MOSAiC drift were analyzed. For this analysis all cyclone centers whose closed isobars encompass the *Polarstern* location were considered. The cyclone tracking algorithm used for this work is based on an algorithm described in Serreze et al. (1993) and Serreze (1995) and updated by Crawford and Serreze (2016). The details of this algorithm can be found in Crawford and Serreze (2016), but a brief description is provided here. The cyclone tracking algorithm was applied to 6-hourly ERA5 MSLP data, interpolated to a 50 km equal area scalable Earth (EASE) grid (Brodzik and Knowles, 2002), consistent with previous applications of this algorithm.

Gridded MSLP, excluding high elevation grid points (higher than 1500 m), are evaluated for minima by comparing each grid point with the surrounding 8 grid points. Each minimum found is then assigned a unique identifier. At the next time period, the MSLP minima are again located and compared with the MSLP minima from 6 hours prior. A given minimum is determined to be a continuation of a previous track if it meets the conditions of where the cyclone may have traveled based on an assumed maximum propagation speed and first guess of where the cyclone would be located 6 hours later. If there is no previous track associated with a minimum, it is defined as a cyclogenesis event and a new cyclone track identifier is created.

For each 6-hourly period the cyclone tracking algorithm identifies the latitude and longitude of all cyclone centers, their area based on the last closed isobar that surrounds the pressure minima, multiple intensity metrics and the unique track identifiers. For this work the MSLP at the center of the cyclone and its depth (defined as the difference between the central pressure and the pressure of the last closed isobar) are used to define each cyclone's intensity. The maximum ERA5 10 m wind speed within each cyclone's area is used as an additional intensity metric. Monthly cyclone statistics (median, IQR, minimum and maximum values) are calculated for the number of cyclone centers whose closed isobars encompass the *Polarstern*, cyclone central MSLP, cyclone depth, cyclone area maximum 10 m wind speed, and *Polarstern* MSLP and wind speed for each cyclone occurrence. These statistics for the MOSAiC year are compared with the same statistics for the 1979-2019 period.

It is possible that multiple minima of MSLP are present within the identified cyclone area. If this is the case, the cyclone is referred to as a multi-center cyclone and each minimum is tracked, although they will all have the same cyclone area, defined by the last closed isobar that encircles the minima. For this work, each MSLP minima that is part of a multi-center cyclone is treated as a separate cyclone event and will have unique latitude, longitude central pressure and depth, but will have the same cyclone area maximum wind speed and *Polarstern* MSLP and wind speed.

Statistics for each cyclone track impacting the MOSAiC drift were recorded and are described in Section 3.2 and listed in the supplementary material (Tables S1 to S12, Figure S2) to serve as a reference for future synoptic studies.

2.3 Indices for large-scale atmospheric circulation

To provide a broader context for the near-surface conditions that occurred during the MOSAiC expedition, the large-scale atmospheric circulation, based on geopotential heights at 250 hPa and 500 hPa (Z250, Z500) as well as monthly teleconnection indices are included in this study. Here, we consider the key teleconnections for the Arctic region, namely the Arctic Oscillation (AO) pattern and the Arctic Dipole (AD) pattern. We derived these patterns and their respective indices from an Empirical Orthogonal Function (EOF) analysis of monthly MSLP anomaly in the three-month period centered on the considered month over 50-90°N. This domain is larger than that used in most studies analyzing the AD pattern in winter (e.g., Wu et al., 2006) or summer (e.g., Cai et al., 2018), but ensures that the domain boundaries do not induce an artificial preference of certain pattern structures (see, e.g. the discussion in Legates, 2003 and Overland and Wang, 2010). In all months, the AO pattern has been identified as the first EOF, whereas the AD pattern occurred as the second, third or fourth EOF pattern. The latter underlines that the AD pattern is less stable than the AO, nonetheless, several studies have shown its critical importance for the Arctic circulation and sea-ice decline (e.g., Wu et al., 2006; Cai et al., 2018; Watanabe et al., 2006; Zhang, 2015). The corresponding AO and AD spatial patterns are shown in Figure S3 exemplarily for the mid-month of each season, i.e. January, April, July and October. The base period for the pattern calculation is 1979-2020 to account for recent changes in the structure and amplitude of the teleconnection patterns.

3. Results

3.1 Near-surface meteorological conditions

3.1.1 Anomalous conditions over the annual cycle

Overall, the full time series of the near-surface meteorological variables (Figure 1) and surface radiative fluxes (Figure 2) indicate that the conditions during MOSAiC were mostly within the recorded minimum-maximum range of the preceding 41 years. This applies also for the frequently occurring storms and moisture intrusion events, which show their clear signatures in the timeseries of MSLP, wind, temperature, TCWV and radiation. However, the figures also highlight that there were frequently conditions over short periods associated with synoptic-scale events that emerge as unusual by being outside of the IQR or were record-breaking. To put that in a monthly context, Table 1 highlights those specific months and variables when two-thirds of the hourly data were outside of the IQR, which we classify as being 'particularly' anomalous monthly conditions. Table 1 shows that for most variables and most months between one third and two thirds of the hourly data during MOSAiC were within the IQR, and here we consider this to be 'normal'. If more than two-thirds of the hourly data during MOSAiC were within the IQR we define this as being 'particularly' normal and note that only a few variables / months show these conditions. Furthermore, a ranking of the monthly and daily mean data of all years 1979-2020 (Figure 3) identifies the several record conditions along the MOSAiC track position. To put the anomalous conditions during MOSAiC as a whole in the context of interannual variability, i.e. to estimate how many periods of particularly anomalous conditions are normal per year, we calculated the occurrence of 'outside IQR' conditions for past nine years (2010-2019, Table S13). If we compare the occurrence of particularly anomalous conditions during MOSAiC (Table 1) with the average over the past nine years (synonymously for the 'recent new Arctic'), it becomes clear that the MOSAiC year was unusual with respect to emerged anomalous TCWV and air temperature. For those more than twice as many conditions outside of the IQR over the year occurred compared to the average conditions.

In order to evaluate changes in Arctic extremes in the recent past the 5th and 95th percentiles for surface meteorological conditions (Figure 1) and surface radiative fluxes and energy budget (Figure 2) have been calculated for the decade 2010-2019. Comparison of these recent decade percentiles to those calculated for the 1979-2019 period reveal a clear shift of the extreme minimum temperature (5th percentile) towards warmer temperatures and frequently higher maximum temperature (95th percentile) particularly during autumn-winter, compared to the long-term statistics (Figure 1). But, the classification of specific MOSAiC conditions as 'normal' or 'anomalous', as discussed below, still persists based on the recent 2010-2019 period (Figures 1 and 2).

3.1.2 Anomalous low pressure in winter-spring

The MSLP during the MOSAiC winter and early spring (January to April 2020) was often in the lowest quartile of MSLP values of the previous four decades (Figures 1 and 4). In the monthly context, the MOSAiC median MSLP for those months is shifted towards smaller MSLP compared to the long-term median. In February-April, the MOSAiC median MSLP was lower than the 25th percentile from the climatology (Figure 4), and the largest shift by ca. 20 hPa occurred in March. Furthermore, in February and March, more than 70% of the hourly MSLP data were outside of the IQR (below the 25th percentile; Table 1), which we define as 'particularly' anomalous. During February-March 2020, the MSLP was extremely anomalously low during almost the entire month (Figure 1), associated with frequent cyclone occurrence (section 3.2) and an extreme positive AO phase (section 3.3). The monthly mean MSLP in the central Arctic showed an anomaly of more than -15 hPa (Figure 5) and was along the MOSAiC track record-breaking, namely the top/3rd lowest pressure for February/March months in the

climatology (Figure 3). Similarly, the April 2020 monthly MSLP anomaly was as low as -15 hPa over the central Arctic (Figure 5). The monthly mean MSLP along the track was anomalously low with the 5th lowest pressure (Figure 3), associated with the impact of a moisture intrusion event (discussed in the next section).

3.1.3 Anomalous warm/moist and cold/dry conditions

Autumn-Winter

October 2019, the first month of MOSAiC, started with normal monthly mean near-surface meteorological conditions (Table 1, Figure 3), but this occurred as conditions varied from anomalously positive T2M, MSLP, TCWV, LWD at the beginning of the month, followed by negative and then again positive anomalies compared to the previous decades (Figures 1 and 2). However, in all months from October 2019 to January 2020, the coldest temperatures shifted towards warmer temperatures, i.e. extreme cold temperatures did not occur as in the past (Figure 4). In December and January, the IQR was reduced compared to previous decades. Temperatures from ca. -25°C to -20°C (248 K to 253 K) occurred more frequently, but extreme warm temperatures above -15°C (258 K) were absent, compared to the previous 4 decades.

The normal mean November conditions (Figure 3, Table 1) come due to canceling effects of two anomalous cold and warm periods. The first ten days in November 2019 were anomalously cold (Figure 1) and ranked among the coldest seven, compared to the climatology; Nov.10 was even the 3rd coldest of the daily climatology (Figures 1 and 3). The relative cold temperatures are related to the negative phase of the AO in November 2019 (section 3.3). The anomalously warm conditions in mid-November were triggered by a strong storm event consisting of two cyclones passing over the MOSAiC track during ca. Nov. 16-20 (Figures 1 and S2, Table S2) associated with a prominent moisture intrusion transporting warm, moist air from the northern North Atlantic into the Arctic. This brought extreme warm temperature anomalies of ca. 15 K, such that the temperature was not only outside of the IQR but also higher than the 95th percentile. These days were classified as being among the six warmest of the climatological record; Nov. 18-19 were the 3rd warmest and Nov. 20 was the 2nd warmest in the climatology for those days. The associated moist anomalies of ca. 5 kg/m^2 (Figure 1) were also extremely anomalous with TCWV above the 95th percentile. The TCWV of those days were classified as being among the seven highest values in the climatology. Nov. 19-20 had record-breaking TCWV, Nov. 21 the 2nd highest and Nov. 16 the 3rd highest (Figure 3). Associated with these warm, moist conditions, the longwave radiative fluxes at the surface were also extremely anomalous. The downward longwave radiation during that event was among the seven highest in the climatology. For downward longwave radiation, Nov. 19-20 had the 2nd highest and Nov. 16 the 3rd highest values of the daily climatology, and the net longwave radiation indicates the extremely low radiation loss into space (Figures 2 and 3).

The dominating event for the anomalous warming in December was also associated with an intrusion of warm, moist air that occurred at the beginning of December (Dec 3-5, 2019; Figure 1), but this event was not associated with a cyclone directly impacting the MOSAiC drift track. This was a shorter-lived event that originated from northwestern Siberia. The temperature at MOSAiC was anomalous, at the edge of the 95th percentile, and ranked as the 5th warmest period in the climatology. The TCWV during this event was extremely anomalous. Dec. 3 and 5 ranked as the 4th highest, while Dec.4 had the 2nd highest TCWV in the daily climatology (Figure 3). The longwave and net radiation (Figure 2) was similarly extremely anomalous as for the November event.

The third anomalous winter warming event occurred in mid-February (Feb. 18-22, 2020; Figure 1) again triggered by an intrusion of warm, moist air from northwestern Siberia into the Arctic. This caused similar anomalous temperature, TCWV and radiation as described above. As with the other two, this event is clearly identified as an event with hourly/daily extremely anomalous

temperature, TCWV and longwave radiation, based on the ERA5 climatology. The near record-breaking days were Feb.19-20, classified as the 5th-4th for temperature and as the 3rd-4th for TCWV (Figure 3). Importantly, the mean February above-normal temperatures at the near surface (Figure 5) and at 850 hPa height (Figures S4 and S5) covers the whole Eastern Arctic region and were influenced by the record-breaking positive AO phase (section 3.3).

Spring

Early March was characterized by unusually cold conditions (Figures 1 and S4) outside of the prior decades' IQR. The near-surface air temperature of the first five days were among the five coldest of the record (Figure 3), while the 850 hPa temperature, including the following five days, were among the 10 coldest. Accordingly, the TCWV was in the first days of March anomalously low (Figure 1) with record low values during March 4-5 showing the second lowest value of the climatological record for those days. Starting in mid-March the temperature mostly remained within the IQR, indicating relatively normal conditions for this time of year (Table 1). In the monthly mean, March 2020 was characterized by slightly below-normal temperatures at the near surface (Figure 5) and at 850 hPa height (Figure S5). This was embedded in a regional cold anomaly with the center over the Fram Strait region, which was linked with anomalous northerly winds (Figure 6) bringing cold polar air into that region (Figure 5) and also led to the rapid southward drift of the MOSAiC floe. (Note: Wind roses for all months are shown in Figure S6). This was associated with the strong negative MSLP anomaly over the Arctic Ocean (Figure 5; see section 3.1.2) related with the positive AO phase (section 3.3) and frequent cyclone occurrence to the south and east of the MOSAiC drift track (section 3.2).

In spring, the MOSAiC expedition experienced a few other records. Above-normal monthly mean temperatures occurred over the whole Arctic Ocean in April and May 2020 with a maximum warm anomaly over northwestern Siberia (Figures 5 and S5). The all-time warmest May temperature in the 1979-2020 ERA5 record was noted in May 2020 (Figure 4).

The monthly mean MOSAiC-trajectory temperature of April 2020 was not unusual, but ranked among the warmest 12 Aprils in the climatology due to southerly warm air advection bringing extreme warm temperatures that occurred during April 15-21, 2020 (Figure 1). This warming was preceded by a brief cold period, with temperatures in the lowest quartile of the record associated with northerly winds (Figure 6). The associated temperature jump was extreme (ca. +20 K) such that the temperature during the specific warm days was record-breaking compared to the climatology (Figures 1 and 3). The temperature on April 16 and 19 was the highest ever and on April 18 and 20 it was the 2nd highest for those days' records. The event was associated with record-breaking moisture (April 16, 19-20 had all-time highest TCWV for those days) and longwave radiation (April 19 had the 2nd lowest and April 20 had the lowest ever net longwave radiation loss on these dates) (Figures 1-3).

In May 2020 the monthly mean MOSAiC temperature was among the six warmest in the full record (Figure 3), which was caused by the anomalous warm temperatures in the second half of May when daily record-breaking temperatures occurred during days 17, 25-29 (Figures 1, 3, 4, and S4). The temperature distribution for this month clearly shows a significant shift of the median (out of the IQR) and, as stated above, had the all-time warmest May temperature (Figures 4 and S4). Associated with the anomalous warm conditions, the monthly mean TCWV was the all-time highest for May over the past four decades (Figure 3). This is consistent with a changed TCWV distribution, which is shifted towards a higher median (out of the IQR) and is flatter and broader (indicated by the significantly larger IQR box) (Figure 4). Table 1 supports the classification as particularly anomalous conditions as more than two-thirds of the hourly temperature and TCWV data in May 2020 were outside of the IQR. A cyclone event that occurred around mid-May (Figure S2, Table S8) caused record-breaking conditions during

those days (Figure 3) that resulted in daily temperatures that were among the 3rd highest in the ERA5 climatology. May 17 showed the highest ever recorded temperature for that day. In addition, the moisture was extremely anomalously high, e.g. the TCWV on May 14-15 ranked as the 3rd highest of the climatological record.

Summer

During summer, 2 m air temperatures near the melting point of ice persisted from late May until early September during MOSAiC. This period of near melting point conditions was more than a month longer than the 1979-2019 median (Figure 1) and is consistent with lower than normal sea-ice concentration along the MOSAiC drift track during the summer (Krumpen et al., 2021). The MOSAiC temperatures in July and August 2020 were especially anomalous (Table 1, Figures 1, 4, and S4) and the warmest of the 1979-2020 period (Figure 3). This is also clearly shown by the shift of the temperature distribution to warmer temperatures with the MOSAiC year's median temperature higher than the long-term 75th percentile (Figures 4 and S4). These record warm conditions near the *Polarstern* were embedded in large positive air temperature anomalies (up to 8 K) over the whole central Arctic (Figure S5). Furthermore, associated with the extreme warm conditions, the whole MOSAiC summer was moister than the climatological mean with daily TCWV anomalies of up to ca. 30 kg/m^2 (Figure 1). The TCWV distributions are significantly shifted towards higher median values for all summer months of June-September 2020, compared to the long-term median (Figure 4). The most anomalous conditions occurred in July-August, when both the median and the 25th percentile exceed the long-term 75th percentile. Along the MOSAiC track, both July and August 2020 show all-time highest monthly TCWV (Figure 3) with 73 and 88% of the hourly TCWV values in these months lying outside of the IQR (Table 1). Further, the all-time highest monthly hourly TCWV in the ERA5 record from 1979-2020 was observed in both June and August (Figure 4). In addition, positive monthly anomalies of ca. 4 kg/m^2 with respect to the climatology occurred over the whole central Arctic region (Figure 5). Finally, two distinct warm air mass intrusion events stand out in middle of September, associated with rapid moisture and temperature increase (above the melting point) and record-breaking values (Figure 1). This implied a temporary positive surface energy budget, i.e. hours of melt conditions of the snow-ice surface (Figure 2).
The anomalous summer (May-September) conditions can be related to the changing sea ice. In earlier years, MOSAiC would have been deep in the ice pack, while in recent years the sea-ice extent is greatly reduced (e.g., Stroeve and Notz, 2018). Accordingly, MOSAiC was closer to the sea-ice edge (e.g., with a distance less than 200 km at the beginning of July; Krumpen et al., 2021) than earlier in the climatology, which is generally linked with warmer and wetter conditions.

3.2 Cyclone activity

Many of the anomalous meteorological conditions discussed in the previous section were associated with cyclone events impacting the MOSAiC drift. The number of cyclone centers, based on 6-hourly data, whose closed isobars included the *Polarstern* drift from October 2019 to September 2020 are compared to the median, IQR and minimum and maximum range of monthly cyclones for the 1979 to 2019 period (Figure 7a). Cyclone counts were below the long-term monthly median counts from October 2019 through January 2020, with less than 12 6-hourly cyclone occurrences impacting the MOSAiC drift in each of these four months. Cyclone counts were near or above the 75th percentile in February and March 2020, consistent with the persistently low pressure observed during these months (Figures 1, 4 and 5). Cyclone counts were near the long-term median in April, with counts well above the long-term median in May and June 2020. Low cyclone numbers were again observed in July and August, with counts near or below the 25th percentile in these months. This is in accordance with the positive MSLP

anomaly over the central Arctic, which was as high as +10 hPa in July and +5 hPa in August (Figure 5). The MOSAiC year ended with very high cyclone counts in September 2020.

Cyclone intensity, as characterized by cyclone central MSLP and depth, as well as MSLP at the *Polarstern*, highlight the anomalous conditions during late winter and early spring 2020, with less unusual conditions for the remainder of the MOSAiC year (Figures 7b, 7c, and S6). MOSAiC year cyclone central MSLP was above the long-term 75th percentile in October and near the long-term median in November 2019. MOSAiC year cyclone central MSLP was then below the long-term median from January to April 2020, with the MOSAiC year median being below the long-term 25th percentile from February to April 2020 (Figure 7b), indicating much stronger than normal cyclones during these months. MOSAiC year cyclone central MSLP was near the long-term median from May through August with lower values (stronger cyclones) observed in September. The median monthly MOSAiC year cyclone depth and maximum cyclone wind speed (Figures 7c and 7d) are consistent with the monthly variability in cyclone central MSLP discussed above. These three metrics of cyclone intensity indicate that late winter into spring of the MOSAiC year experienced anomalously strong cyclones relative to the prior 40 years. This is consistent with the shift to a record positive AO during winter 2020 (section 3.3). The pressure and wind speed observed at the *Polarstern* during cyclone events (Figure S7) were mostly consistent with the cyclone intensities discussed above, except for the ship cyclone wind speed during March, which was below the long-term median, despite the monthly median wind speed being above the long-term 75th percentile (Figure 4).

For each 6-hourly cyclone occurrence the percentile ranking of each cyclone intensity metric was calculated compared to the 1979-2020 ERA5 data. Cyclone occurrences were classified as strong if the cyclone depth was in the top 25th percentile, normal if the depth was between the 25th and 75th percentiles (i.e. within the IQR), and weak if the depth was in the lowest 25th percentile for each month in the 1979-2020 period. The opposite thresholds were used for cyclone central MSLP to identify strong, normal or weak cyclones. More than 50% of cyclones that impacted the *Polarstern* from February to April 2020 were classified as strong based on their central pressure (Figure 8a), consistent with the low MSLP seen in Figure 1 and the distribution of cyclone MSLP shown in Figure 7b. Ranking the cyclones by depth revealed a similar pattern of an unusually large number of strong cyclones during these late winter and early spring months (Figure 8b). The remainder of the MOSAiC year was characterized by near normal to below normal frequency of strong cyclones and near normal to above normal occurrence of normal or weak cyclones.

Based on the cyclone track information from the Crawford and Serreze (2016) cyclone tracking algorithm, all tracks whose cyclone areas encompassed the MOSAiC drift in each month were identified. For each of these tracks the start and end date and time and location of the track and the start and end date and time of when the cyclone area included the Polarstern were recorded. In addition, the minimum central MSLP, minimum *Polarstern* MSLP, maximum depth, maximum cyclone area 10 m wind speed and maximum *Polarstern* 10 m wind speed when the cyclone area encompassed the *Polarstern* were recorded (Tables S1-S12) to serve as a reference for future synoptic studies. The track locations, for each month of the MOSAiC expedition, are shown in Figure S2.

The anomalous warm and moist events discussed in section 3.1 (Figure 1) can be linked to specific cyclones impacting the MOSAiC drift track. The shift from anomalously warm to cold conditions in mid-November was associated with a cyclone that started in North America on 11 Nov. 2019 and traversed the central Arctic towards Siberia (Figure S2) and whose maximum intensities were in the strongest 25th percentile of all November cyclones since 1979 (Table S2). The shift from anomalously warm to cold conditions in late February was associated with a cyclone track that started on 18 Feb. near Novaya Zemlya (Figure S2) whose maximum intensity was near the strongest 10th percentile (Table S5). The exceptionally low MSLP in March 2020 was associated with 11 separate cyclone tracks from 11 to 25 March impacting the

Polarstern (Figure S2). These cyclones' central MSLP ranked in the top 25th percentile of all March storms from 1979-2019 (Table S6). The location of these cyclones, to the south and east of the *Polarstern*, resulted in persistent northerly winds during mid-March (Figure 6), which caused a rapid southward drift of the *Polarstern* (Krumpen et al., 2021). The warm and moist conditions occurring in mid to late April 2020 were associated with three cyclone tracks impacting the *Polarstern* from 16 to 19 April whose intensities ranked in or near the top 25th percentile, in terms of wind speed at the *Polarstern* and central MSLP (Figure S2, Table S7).

3.3 Large-scale atmospheric circulation

Overall, the monthly time series of the Arctic Oscillation (AO) and Arctic Dipole (AD) teleconnection indices (Figure 9) indicate an unusual course from late autumn 2019 until early spring 2020. A strong negative AO phase in November was followed by a near neutral AO in December. The most striking circulation anomaly of the MOSAiC year develops during winter. The MOSAiC winter (January-March 2020) was characterized by an exceptionally strong and cold polar vortex with Z500 and Z250 anomalies as large as -25 gpm (Figure 10). This was accompanied by a record-breaking positive phase of the AO (Figure 9) and related near-surface warm anomalies over northern Eurasia (which was unprecedented in the MERRA-2 record back to 1980; Lawrence et al., 2020) and cold anomalies in Alaska, northern Canada and Greenland (Figures 5 and S5). Due to its location, MOSAiC was mainly affected by the AO accompanied warming in February (Figures 5 and S5) and accordingly showed above-normal temperatures (Figures 1 and S4; section 3.1). In addition, the center of the Z500 and Z250 circulation anomalies changed its position during winter (Figure 10) due to the impact of the prevailing phase of the AD pattern, which was negative in February, and positive in January and March. The exceptional large-scale flow configuration in February with strong positive AO and strong negative AD is related with the very high cyclone occurrences in that month (Figure 7). Another key feature related to this anomalous atmospheric circulation in winter was the associated anomalous wind, which was experienced by MOSAiC (section 3.1). The wind speed was particularly anomalously high (Figure 4) and the wind direction was particularly anomalous (northerly) in March (Figure 6, Table 1), which pushed the drift more quickly across the transpolar drift.

During the remaining months of the MOSAiC expedition, the large-scale atmospheric conditions were quite normal with not many unusual index values. Only in July a rather strong quasi-barotropic anticyclonic anomaly develops over the Arctic Ocean with positive MSLP anomalies as large as +10 hPa (Figure 5) and Z500 anomalies as large as +20 gpm (Figure 10). These circulation anomalies correspond to the strong negative phase of both the AO and the AD teleconnection patterns.

4. Conclusions

Overall, the MOSAiC expedition represents a changing Arctic with higher temperature and more moisture in particular during summer and more intense winter-spring storms. This relates with the changed background state, often called the 'New Arctic': Compared to earlier years, the *Polarstern* has seen thinner sea ice in winter and lower sea-ice concentration in summer (Krumpen et al., 2021). The main findings for the meteorological conditions along the yearlong MOSAiC track based on ERA5 reanalysis data and compared to the past four decades are:

- For most variables and months, the MOSAiC conditions were fairly typical: The hourly and daily near-surface meteorological variables and surface radiative fluxes during MOSAiC were mostly within the recorded IQR of the preceding four decades. For most variables and months up to two-thirds of the hourly MOSAiC data were inside of this IQR. Most of the MOSAiC year's monthly median values were also within the IQR. Unusual were the significantly higher wind speed in March, the lower MSLP in February-April, and the

higher temperature and TCWV in May-August, with the all-time hourly record high temperature in May and TCWV in June and August.

- The conditions at MOSAiC were impacted by a series of interesting extreme events, such as extreme storm (exceptional strong wind speed and low pressure) and moisture intrusion (exceptional high total column water vapor) events. Those show a clear signature in the temperature and moisture data, which were classified not only as unusual (by being out of the IQR), but as extremely anomalous (by being larger than the 95th percentile) or even record-breaking considering the long-term statistics. The most noteworthy events, associated with extreme warm and moist conditions, occurred from late fall until early spring in mid-November, the beginning of December, mid-February, mid-April, and mid-May. In winter, these events were associated with extremely anomalous downward and net longwave radiation at the surface.
- The number of cyclones and their intensity were anomalous during the MOSAiC winter and spring, with monthly cyclone counts well above the long-term median from February through June 2020. The cyclones in the period from late winter to spring (February to April 2020) were also stronger than normal with more than 50% of cyclone events classified as being strong.
- A list of all cyclone events that impacted the MOSAiC drift is provided and could be further analyzed in follow-up process-oriented studies. Of interest to analyze is for example the coupling between free-troposphere, boundary-layer, and surface processes, and sea-ice impacts during cyclone events (e.g., Persson et al., 2020).
- During summer, the near melting point conditions were more than a month longer than usual (compared to the 1979-2019 median) in accordance with the all-time warmest and wettest mean July and August conditions. These summer record warm and moist conditions occurred not only near the *Polarstern* but over the whole central Arctic.
- Not many record low temperature appeared during MOSAiC, but unusually cold conditions occurred during the beginning of November and early March (linked with extremely anomalous low MSLP), associated with the large-scale atmospheric circulation conditions (AO phase).

References

Ballinger, TJ, Overland, JW, Wang, M, Bhatt, US, Hanna, E, Hanssen-Bauer, I, Kim, SJ, Thoman, RL, Walsh, JE. 2020. Arctic Surface Air Temperature. *Arctic Report Card*. DOI: http://dx.doi.org/10.25923/gcw8-2z06

Box, J, 19 coauthors. 2019. Key indicators of Arctic climate change: 1971-2017. *Environmental Research Letters* 14: 045010. DOI: http://dx.doi.org/10.1088/1748-9326/aafc1b

Brodzik, MJ, Knowles, KW. 2002. EASE-Grid: A Versatile Set of Equal-Area Projections and Grids. Chapter 5 in Michael F.Goodchild (Ed.) *Discrete Global Grids: A Web Book*. Santa Barbara, California USA, National Center for Geographic Information & Analysis. https://escholarship.org/uc/item/9492q6sm.

Cai, L, Alexeev, VA, Walsh, JE, Bhatt, US. 2018. Patterns, impacts, and future projections of summer variability in the Arctic from CMIP5 models. *Journal of Climate* 31: 9815-9833. DOI: http://dx.doi.org/10.1175/JCLI-D-18-0119.1

Crawford, AD, Serreze, MC. 2016. Does the summer Arctic frontal zone influence Arctic Ocean cyclone activity? *Journal of Climate* 29: 4977-4993.

Graham, RM, Hudson, SR, Maturilli, M. 2019a. Improved performance of ERA5 in Arctic gateway relative to four global atmospheric reanalyses. *Geophysical Research Letters* 46: 6138-6147. DOI: http://dx.doi.org/10.1029/2019GL082781

Graham, R, Cohen, L, Ritzhaupt, N, Segger, B, Graversen, R, Rinke, A, Walden, VP, Granskog, MA, Hudson, SR. 2019b. Evaluation of six atmospheric reanalyses over Arctic sea ice from winter to early summer. *Journal of Climate* 32: 4121-4143. DOI: http://dx.doi.org/10.1175/JCLI-D-18-0643.1

Hersbach, H, 42 coauthors. 2020. The ERA5 global reanalysis. *Quarterly Journal of the Royal Meteorological Society* 146(730): 1999-2049. DOI: http://dx.doi.org/10.1002/qj.3803

Krumpen, T, 37 coauthors. 2020. The MOSAiC ice floe: sediment-laden survivor from the Siberian shelf. *The Cryosphere* 14: 2173-2187. DOI: http://dx.doi.org/10.5194/tc-2020-64

Krumpen, T, 15 coauthors. 2021. The MOSAiC Drift: Along-track ice conditions from space and comparison with previous years. submitted to *The Cryosphere*

Lawrence, ZD, Perlwitz, J, Butler, AH, Manney, GL, Newman, PA, Lee, SH, Nash, ER. 2020. The remarkably strong Arctic stratospheric polar vortex of winter 2020: Links to record-breaking Arctic Oscillation and ozone loss. *Journal of Geophysical Research Atmosphere* 125: e2020JD033271. DOI: http://dx.doi.org/10.1029/2020JD033271

Legates, DR. 1993). The effect of domain shapes on principal components analysis: a reply. *International Journal of Climatology* 13: 219-228. DOI: http://dx.doi.org/10.1002/joc.3370130207

Manney, GL, Livesey, NJ, Santee, ML, Froidevaux, L, Lambert, A, Lawrence, ZD, Millán, LF, Neu, JL, Read, WG, Schwartz, MJ, Fuller, RA. 2020. Record- low Arctic stratospheric ozone in 2020: MLS observations of chemical processes and comparisons with previous extreme winters. *Geophysical Research Letters*, 47: e2020GL089063. DOI: http://dx.doi.org/10.1029/2020GL089063

Overland, JE, Wang, M. 2010. Large-scale atmospheric circulation changes are associated with the recent loss of Arctic sea ice. *Tellus A* 62: 1-9. DOI: http://dx.doi.org/10.1111/j.1600-0870.2009.00421.x

Overland, JE, Wang, M. 2020. The 2020 Siberian heat wave. *International Journal of Climatology* 41 (Suppl. 1): E2341-E2346. DOI: http://dx.doi.org/10.1002/joc.6850

Persson, OPG, Shupe, M, deBoer, G, Perovich, D, Haapala, J, Graeser, J, Solomon, A, Cox, C, Hutchings, J. 2020. Structure of Arctic cyclones during MOSAiC and their surface impacts, AGU Fall Meeting, December 1-17.

Serreze, MC. 1995. Climatological aspects of cyclone development and decay in the Arctic. *Atmosphere and Ocean* 33: 1-23, DOI: http://dx.doi.org/10.1080/70559900.1995.9649522

Serreze, MC, Box, JE, Barry, RG, Walsh, JE. 1993. Characteristics of Arctic synoptic activity 1952-1989. *Meteorology and Atmospheric Physics* 51: 147-164. DOI: http://dx.doi.org/10.1007/BF01030491

Shupe, MD, Rex, M, Dethloff, K, Damm, E, Fong, AA, Gradinger, R, Heuzé, C, Loose, B, Makarov, A, Maslowski, W, Nicolaus, M, Perovich, D, Rabe, B, Rinke, A, Sokolov, V, Sommerfeld, A. 2020. The MOSAiC Expedition: A Year Drifting with the Arctic Sea Ice, *Arctic Report Card*, DOI: http://dx.doi.org/10.25923/9g3v-xh92

Stroeve, J, Notz, D. 2018. Changing state of Arctic sea ice across all seasons. *Environmental Research Letters* 13: 103001, DOI: http://dx.doi.org/10.1088/1748-9326/aade56

Watanabe, E, Wang, J, Sumi, A, Hasumi, H. 2006. Arctic dipole anomaly and its contribution to sea ice export from the Arctic Ocean in the 20th century. *Geophysical Research Letters* 33: L23703, DOI: http://dx.doi.org/10.1029/2006GL028112

Wohltmann, I, von der Gathen, P, Lehmann, R, Maturilli, M, Deckelmann, H, Manney, GL, et al. 2020. Near- complete local reduction of Arctic stratospheric ozone by severe chemical loss in spring 2020. *Geophysical Research Letters* 47: e2020GL089547. DOI: http://dx.doi.org/10.1029/2020GL089547

Wu, B, Wang, J, Walsh, JE. 2006. Dipole Anomaly in the winter Arctic atmosphere and its association with Arctic sea ice motion. *Journal of Climate* 19: 210-225, DOI: http://dx.doi.org/10.1175/JCLI3619.1

Zhang, R. 2015. Mechanisms for low-frequency variability of summer Arctic sea ice extent. *Proceedings National Academy of Science USA* 112: 4570-4575, DOI: http://dx.doi.org/10.1073/pnas.1422296112

Funding information. AR and DH acknowledge funding by the Deutsche Forschungsgemeinschaft (DFG, German Research Foundation) - project 268020496 TRR 172, within the Transregional Collaborative Research Center "ArctiC Amplification: Climate Relevant Atmospheric and SurfaCe Processes, and Feedback Mechanisms (AC)3. AR, DH, RJ acknowledge funding by the German Federal Ministry of Education and Research (BMBF) via the project "Synoptic events during MOSAiC and their Forecast Reliability in the Troposphere-Stratosphere System (SynopSys)" with grant 03F0872A. JC and EC acknowledge funding from the United States National Science Foundation grants PLR 1603384 and OPP 1805569.

Acknowledgments. We greatly thank Julius Eberhard and Ida Sigusch for their help with data preparation and graphics that provided the basis for the time series analysis. We thank Matthew Shupe for useful comments that strengthened the paper. We thank ECMWF and DKRZ for providing ERA5 reanalysis data, generated using Copernicus Climate Change Service Information (C3S). This manuscript was produced as part of MOSAiC with the tag MOSAiC20192020 and the Project_ID AWI_PS122_00.

Contributions. Conception, design and initial manuscript draft: AR, JC; Analysis of data: AR, JC, EC, DH; Interpreting data, drafting and revising the article: all authors; Final approve of the version to be submitted: all authors

Competing of interest. The authors have declared that no competing interests exist.

Code/data availability. The position of *Polarstern* is made available by AWI at the dashboard website https://dashboard.awi.de/data-xxl/rest/data?sensors=vessel:polarstern:hydrins_1:latitude&sensors=vessel:polarstern:hydrins_1:longitude&beginDate=2019-09-20T18:00:00&aggregate=minute&limit=10000&streamit=true&withQualityFlags=false&withLogicalCode=false&format=text/csv.
ERA5 data are made available by the Copernicus Climate Change Service (C3S) at https://cds.climate.copernicus.eu/cdsapp#!/home. Copernicus Climate Change Service (C3S) (2017): ERA5. Fifth generation of ECMWF atmospheric reanalyses of the global climate. Copernicus Climate Change Service Climate Data Store (CDS), 2017–2020.

Table 1. Percent of time (%) that each variable was outside of the 1979-2019 interquartile range (IQR) (first row for each variable) and the percent of time (%) being below/above the 25th/75th percentile (second row for each variable) for each month of the MOSAiC trajectory, based on hourly ERA5 data. Variables: MSLP - mean sea level pressure, TCWV - total column water vapor, T2M - 2m air temperature, T850 - 850hPa air temperature, US10 - 10m wind speed, U10 and V10 - 10m zonal and meridional wind components, LWD - longwave downward radiation at the surface, SWD - shortwave downward radiation at the surface, NetRad - net radiation at the surface. Note that the occurrence of SWD is limited during polar night conditions (Oct.-Mar.). Any month with more than 2/3 (66%) of the MOSAiC hourly data of a variable outside of the IQR is highlighted in bold to indicate particularly anomalous conditions. Any month with more than 2/3 of the MOSAiC hourly data of a variable inside of the IQR (i.e. 34% out of IQR) is highlighted in italic and underlined for labeling it as being particularly normal.

	2019			2020								
	Oct.	Nov.	Dec.	Jan.	Feb.	Mar.	Apr.	May	June	July	Aug.	Sep.
MSLP	40 13/27	60 19/41	48 6/42	51 46/5	**73** 73/0	**74** 72/2	65 58/7	38 34/4	45 25/20	*31* 7/24	47 13/34	37 27/10
TCWV	50 12/38	46 17/29	47 1/46	39 5/34	64 24/40	56 28/28	54 20/34	**69** 14/55	57 6/51	**73** 1/72	**88** 1/87	58 17/41
T2m	38 16/22	61 32/29	*26* 7/19	*27* 9/18	48 16/32	*30* 21/9	45 10/35	**73** 10/63	64 20/44	56 4/52	**68** 8/60	47 8/39
T850	52 6/46	60 33/27	54 0/54	*12* 1/11	37 8/29	60 45/15	59 24/35	**69** 15/54	49 8/41	**75** 8/67	**85** 0/85	35 2/33
US10	37 26/11	48 18/30	58 41/17	52 32/20	50 11/39	**67** 19/48	52 16/36	50 17/33	52 22/30	52 26/26	50 32/18	55 30/25
LWD	51 22/28	57 28/29	*33* 6/27	38 9/29	61 27/34	38 15/23	58 23/35	65 12/53	63 9/54	**69** 8/61	**84** 2/82	51 15/36
U10	43 32/11	52 35/17	53 13/40	59 41/18	61 50/11	57 11/46	56 12/44	**67** 52/15	42 16/26	**67** 60/7	*30* 25/5	53 30/23
V10	41 30/11	64 43/21	50 33/17	42 23/19	50 20/30	**68** 60/8	61 37/24	55 21/34	61 36/25	44 38/6	59 15/44	47 14/33
SWD	-	-	-	-	-	48 16/32	60 28/32	50 34/16	55 44/11	45 31/14	**79** 71/8	58 51/7
NetRad	57 23/34	55 23/32	40 6/34	46 10/36	65 34/31	52 15/37	62 25/37	50 29/21	50 23/27	46 19/27	**71** 18/53	56 23/33

Figures titles and legends

Figure 1: Comparison between MOSAiC and climatological near-surface meteorological conditions. The comparison presents time series of a) mean sea level pressure (hPa), b) 10m wind speed (m/s), c) 2m air temperature (K), and d) total column water vapor (kg/m^2) at *Polarstern* position and based on ERA5 (average over the four nearest grid points). Red line: MOSAiC year, black line: median over 1979-2019, dark grey shading: interquartile range, blue lines: 5th and 95th percentiles, light grey shading: min-max range from 1979-2019 data. The 5th and 95th percentiles from the recent 2010-2019 period are shown with green lines and indicate the full range of this period's data. Based on hourly data, 24 hour running means are plotted. Note: The abrupt decrease of the wind speed and changes in the range of variability of temperature at the beginning of June is associated with the parking of *Polarstern* in the ice-free fjord of Svalbard between MOSAiC leg 3 and leg 4 and the associated sheltering.

Figure 2: Comparison between MOSAiC and climatological surface energy fluxes. The comparison presents time series of surface fluxes (W/m^2) of a) downward shortwave radiation, b) downward longwave radiation, c) net radiation, and d) surface energy budget (SEB) at *Polarstern* position and based on ERA5 (average over the four nearest grid points). Red line: MOSAiC year, black line: median over 1979-2019, dark grey shading: interquartile range, blue lines: 5th and 95th percentiles, light grey shading: min-max range from 1979-2019 data. The 5th and 95th percentiles from the recent 2010-2019 period are shown with green lines and indicate the full range of this period's data. Based on hourly data, 24 hour running means are plotted. Note: The abrupt increase of net radiation (and thus SEB) at the beginning of June is associated with the parking of *Polarstern* in the ice-free fjord of Svalbard between MOSAiC leg3 and leg4. The abrupt decrease of SEB at the end of September is associated with temporarily reduction of sea-ice concentration near the ice edge in the Fram Strait and large upward turbulent heat fluxes.

Figure 3: Ranking of near-surface meteorological parameters during MOSAiC in context of the past four decades. The ranking is presented for monthly and daily mean data based on the full record of 1979-2020 for a) mean sea level pressure, b) 2m air temperature, c) total column water vapor, and d) surface net radiation at *Polarstern* position and based on ERA5 (weighted average over the four nearest grid points). Darkest red/blue: MOSAiC year had the highest/lowest value out of the past years data. The timestamp (start of the month) is given along the drift position.

Figure 4: Monthly comparison of near-surface meteorological conditions between MOSAiC and climatology. The comparison shows monthly median (red line), 25th and 75th percentile (box) and minimum and maximum (whiskers) of mean sea level pressure (hPa), 10m wind speed (m/s), 2m air temperature (K), total column water vapor (kg/m^2), and surface net radiation (W/m^2) for the MOSAiC year (right box and whisker plots) and for ERA5 1979 to 2019 (left box and whisker plot).

Figure 5: Spatial anomalies of monthly near-surface meteorological conditions during MOSAiC. Monthly anomaly of 2m air temperature (color shading; K), mean sea level pressure (black isolines; hPa), and total column water vapor (green isolines; kg/m^2; only plotted for anomalies $\geq \pm 2$ kg/m^2) for the MOSAiC year, compared to the previous four decades. The MOSAiC drift trajectory in the specific month is included as mangenta line.

Figure 6: Comparison of wind direction between MOSAiC and climatology for spring. The wind direction distribution shown as wind roses for March and April. Red filled: MOSAiC year, black encircled: 1979-2019. Based on hourly data. The other months of the year are shown in the Supplemental Material (Figure S6).

Figure 7: Monthly cyclone statistics comparison between MOSAiC and climatology. The cyclone statistics shows (a) Monthly count of 6-hourly cyclone occurrence for the MOSAiC year of October 2019 to September 2020 (red asterisks) and median (red line) with 25th and 75th percentile (box) and minimum and maximum (whiskers) for ERA5 from 1979-2019. (b-d) Monthly median (red line), 25th and 75th percentile (box) and minimum and maximum (whiskers) of (b) cyclone central pressure, (c) cyclone depth and (d) maximum cyclone 10 m wind speed for the MOSAiC year (right box and whisker plots) and for ERA5 1979 to 2019 (left box and whisker plots).

Figure 8: Characteristics of cyclone strength during MOSAiC. Frequency of occurrence (%) of weak (blue), normal (grey), and strong (red) cyclones based on a) cyclone central pressure and b) cyclone depth during each month of the MOSAiC year from October 2019 to September 2020. Cyclone intensity is defined as weak if the central mean sea level pressure MSLP (depth) is in the top (bottom) 25th percentile, normal if the central MSLP (depth) is within the IQR and strong if the central MSLP (depth) is in the bottom (top) 25th percentile.

Figure 9: Teleconnection indices for the MOSAiC year. Monthly indices of Arctic Oscillation (AO) and Arctic Dipole (AD) for October 2019 to September 2020. Based on ERA5 data. The corresponding spatial patterns are shown in Figure S3.

Figure 10: Monthly anomalies of atmospheric circulation during MOSAiC. The circulation anomalies are presented by monthly anomaly of 500 hPa geopotential height (color shading; gpm) and 250 hPa geopotential height (isolines; gpm) for the MOSAiC year, compared to the previous four decades. The MOSAiC drift trajectory in the specific month is included as mangenta line.

Figure

Click here to access/download;Figure;meteo-fig.pdf

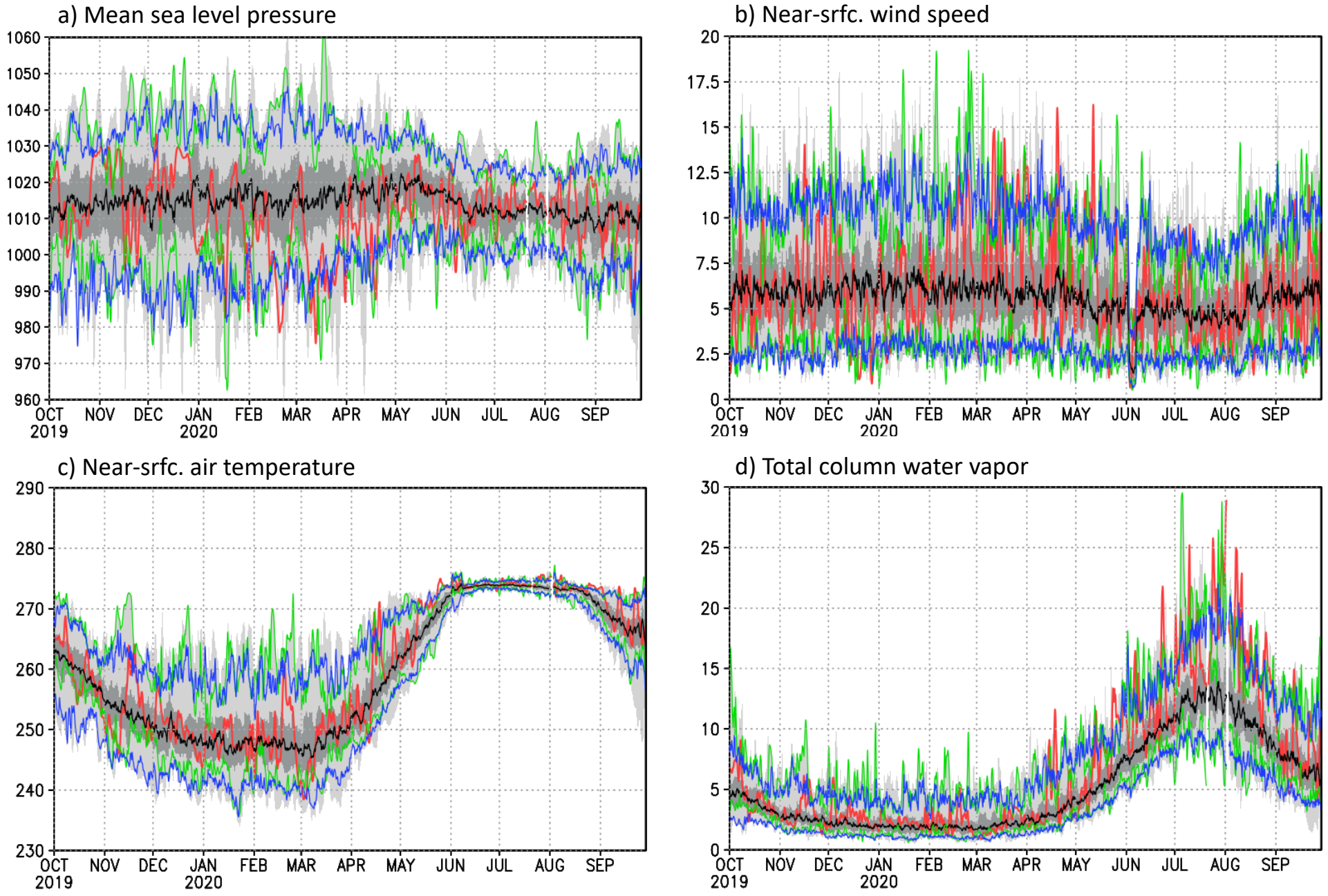

Figure 1.

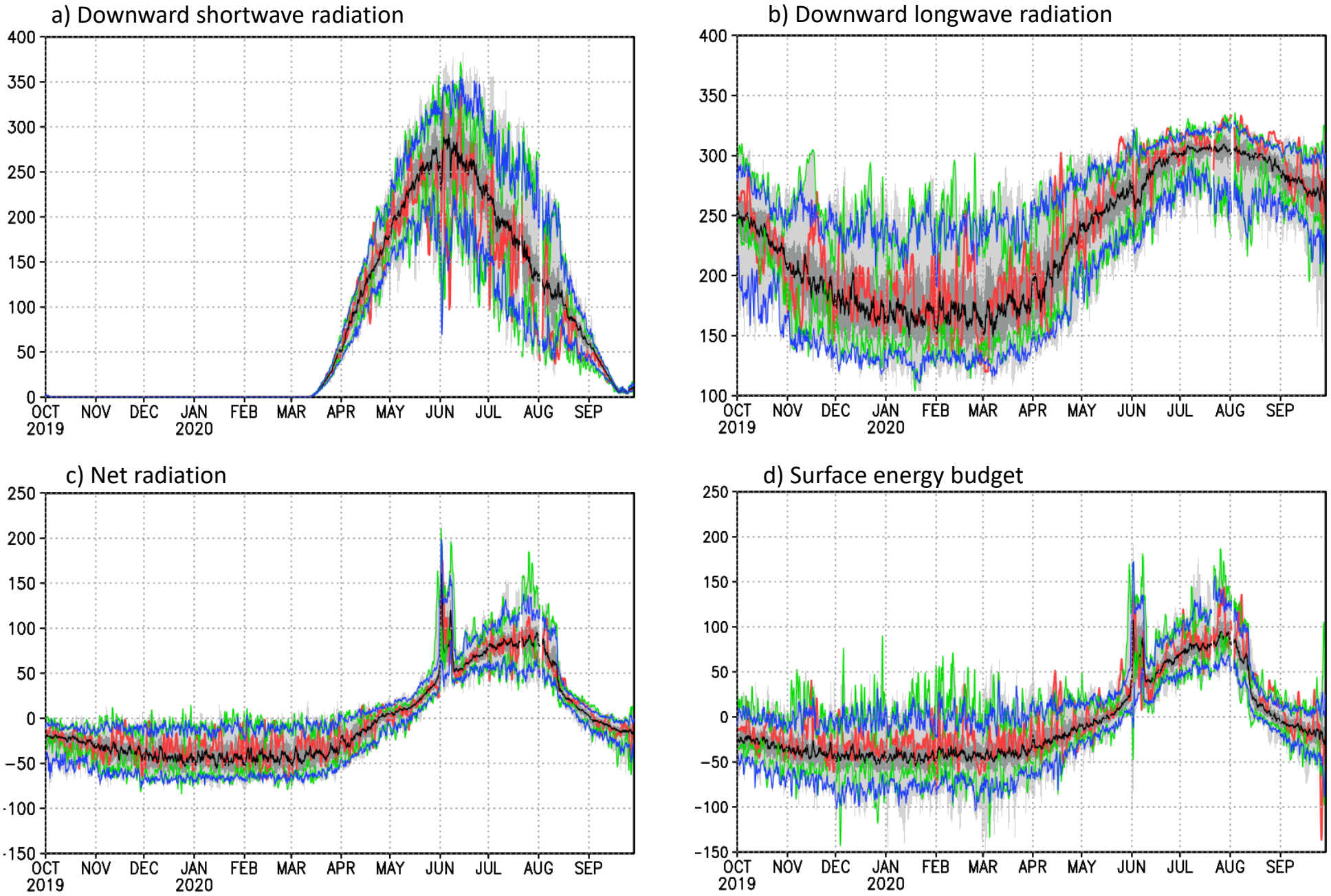
a) Downward shortwave radiation
b) Downward longwave radiation
c) Net radiation
d) Surface energy budget
OCT 2019
NOV
DEC
JAN 2020
FEB
MAR
APR
MAY
JUN
JUL
AUG
SEP

Figure 2.

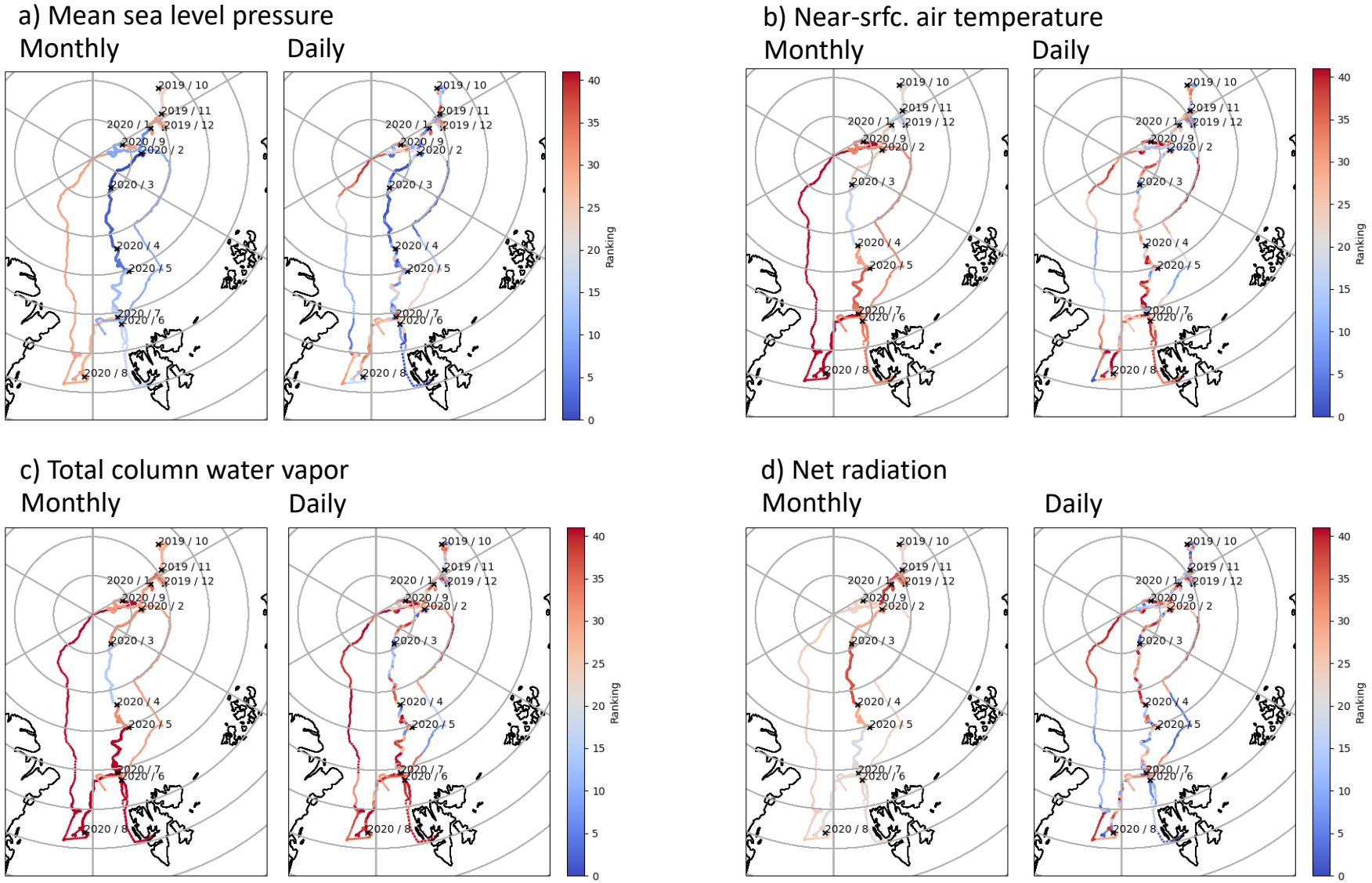
a) Mean sea level pressure
Monthly
Daily
b) Near-srfc. air temperature
Monthly
Daily
c) Total column water vapor
Monthly
Daily
d) Net radiation
Monthly
Daily
2019 / 10
2019 / 11
2019 / 12
2020 / 1
2020 / 2
2020 / 3
2020 / 4
2020 / 5
2020 / 6
2020 / 7
2020 / 8
2020 / 9
Ranking
0
5
10
15
20
25
30
35
40

Figure 3.

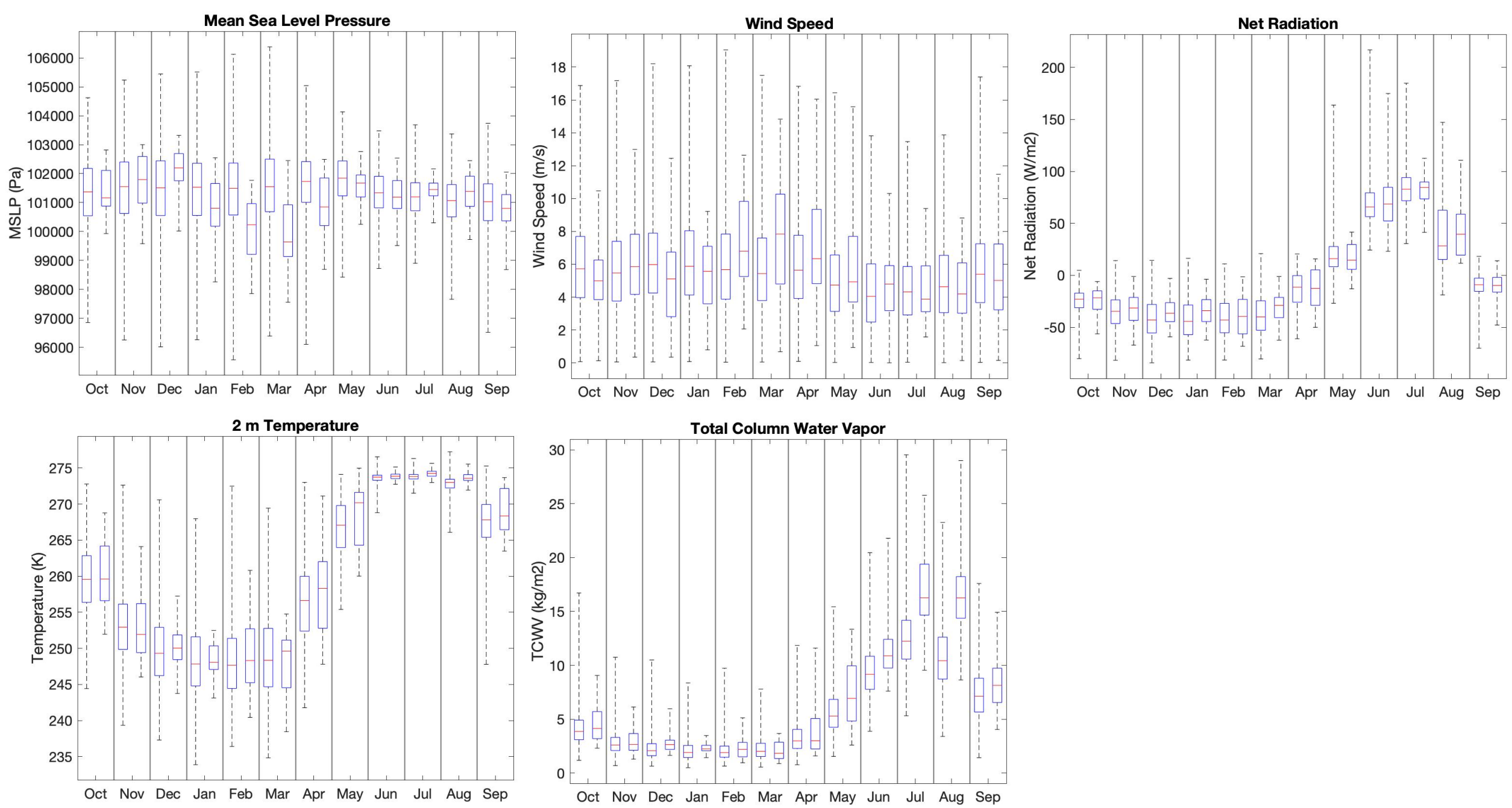
Mean Sea Level Pressure
MSLP (Pa)
106000
105000
104000
103000
102000
101000
100000
99000
98000
97000
96000
Oct Nov Dec Jan Feb Mar Apr May Jun Jul Aug Sep
Wind Speed
Wind Speed (m/s)
18
16
14
12
10
8
6
4
2
0
Oct Nov Dec Jan Feb Mar Apr May Jun Jul Aug Sep
Net Radiation
Net Radiation (W/m2)
200
150
100
50
0
-50
Oct Nov Dec Jan Feb Mar Apr May Jun Jul Aug Sep
2 m Temperature
Temperature (K)
275
270
265
260
255
250
245
240
235
Oct Nov Dec Jan Feb Mar Apr May Jun Jul Aug Sep
Total Column Water Vapor
TCWV (kg/m2)
30
25
20
15
10
5
0
Oct Nov Dec Jan Feb Mar Apr May Jun Jul Aug Sep

Figure 4.

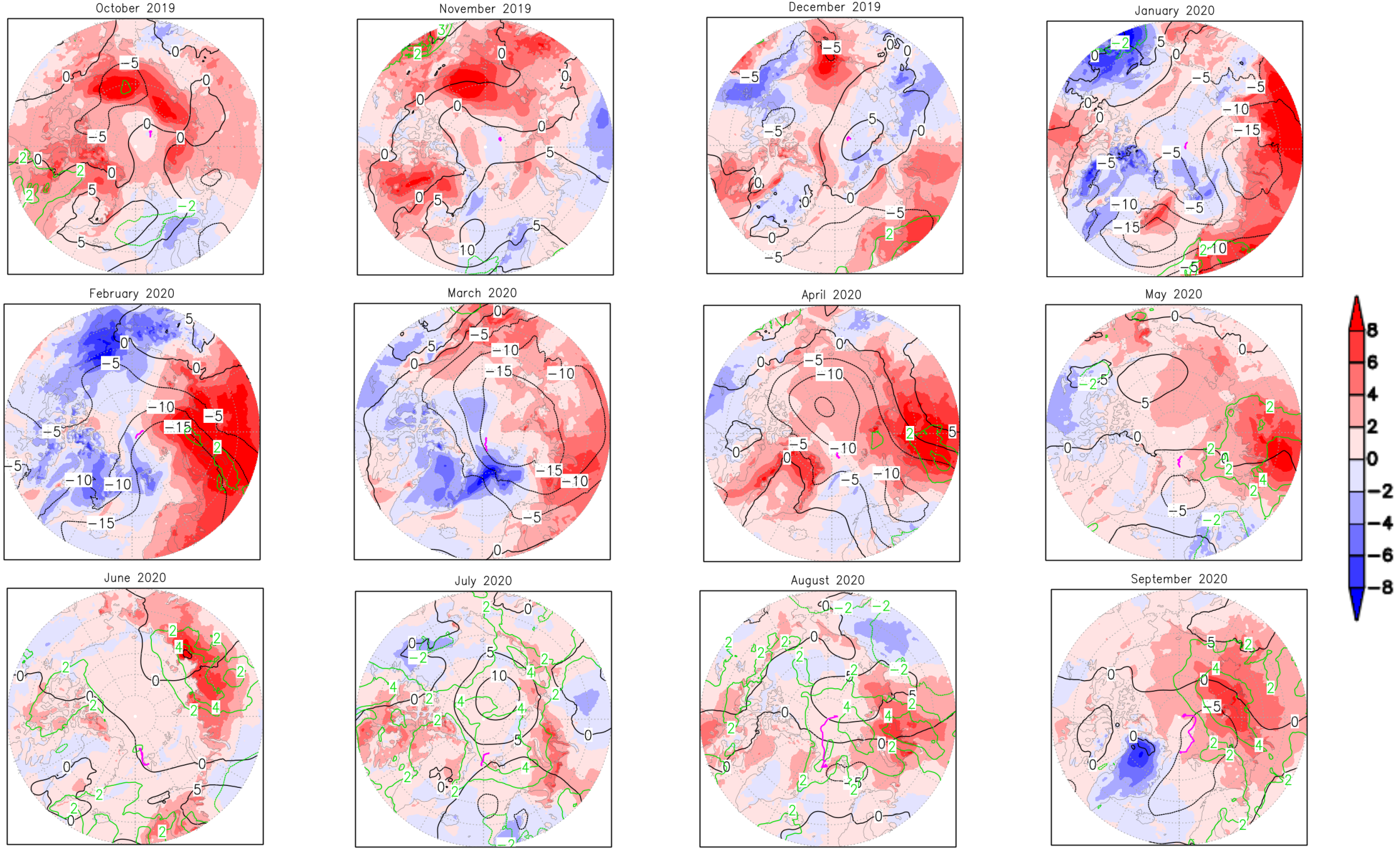
October 2019
November 2019
December 2019
January 2020
February 2020
March 2020
April 2020
May 2020
June 2020
July 2020
August 2020
September 2020
8
6
4
2
0
−2
−4
−6
−8

Figure 5.

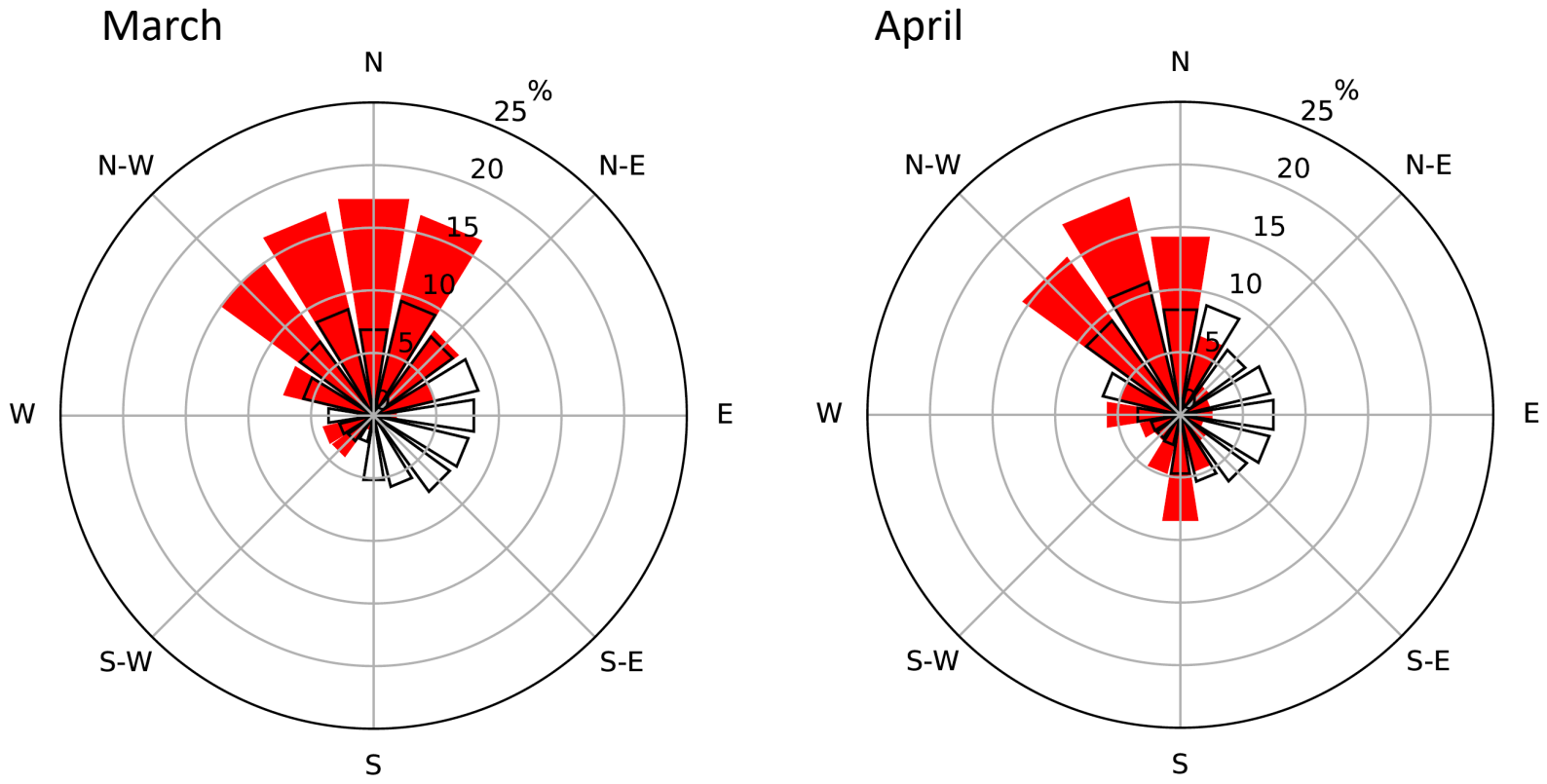

Figure 6.

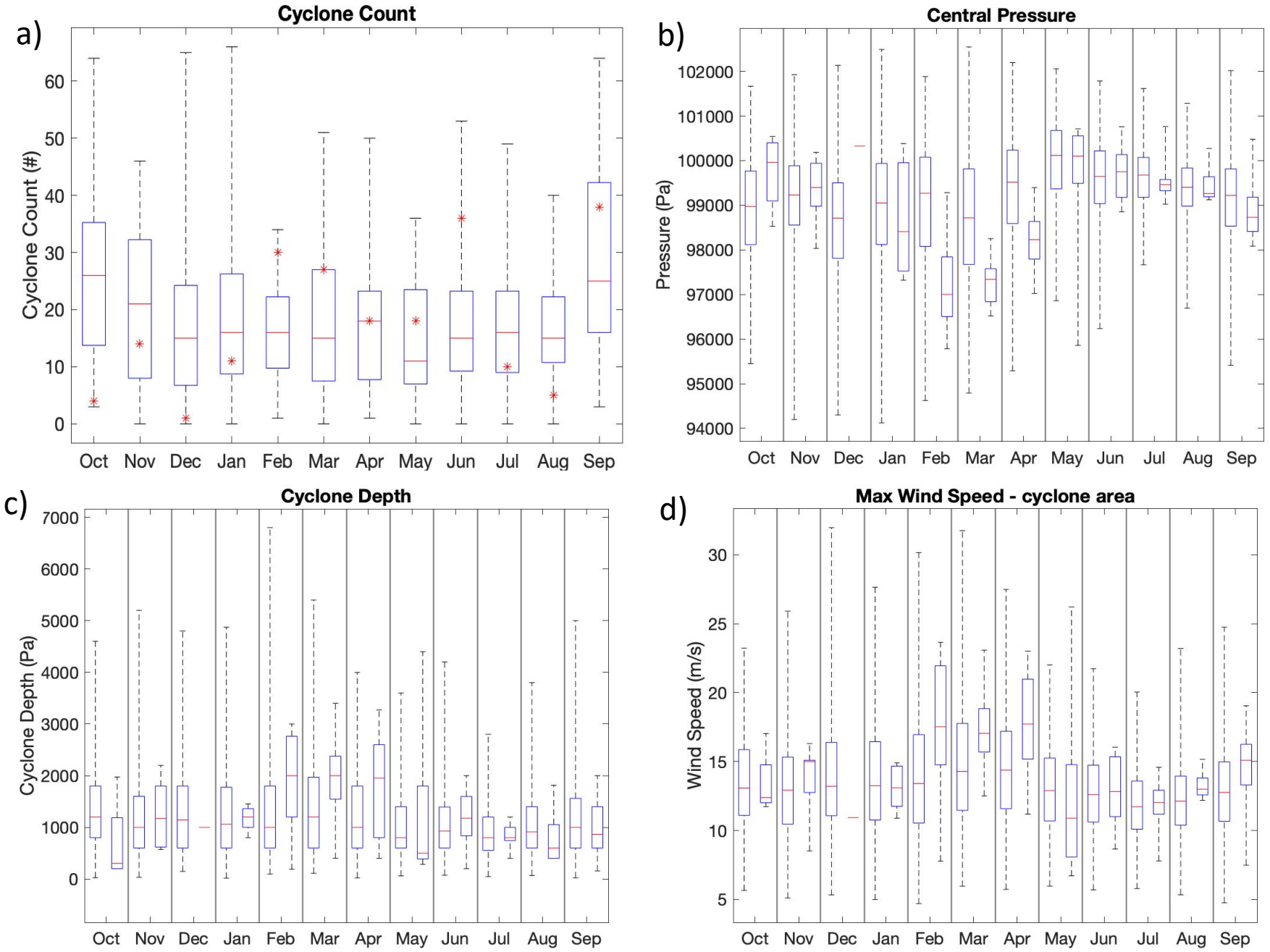
a)
Cyclone Count
Cyclone Count (#)
0
10
20
30
40
50
60
Oct Nov Dec Jan Feb Mar Apr May Jun Jul Aug Sep
b)
Central Pressure
Pressure (Pa)
94000
95000
96000
97000
98000
99000
100000
101000
102000
Oct Nov Dec Jan Feb Mar Apr May Jun Jul Aug Sep
c)
Cyclone Depth
Cyclone Depth (Pa)
0
1000
2000
3000
4000
5000
6000
7000
Oct Nov Dec Jan Feb Mar Apr May Jun Jul Aug Sep
d)
Max Wind Speed - cyclone area
Wind Speed (m/s)
5
10
15
20
25
30
Oct Nov Dec Jan Feb Mar Apr May Jun Jul Aug Sep

Figure 7.

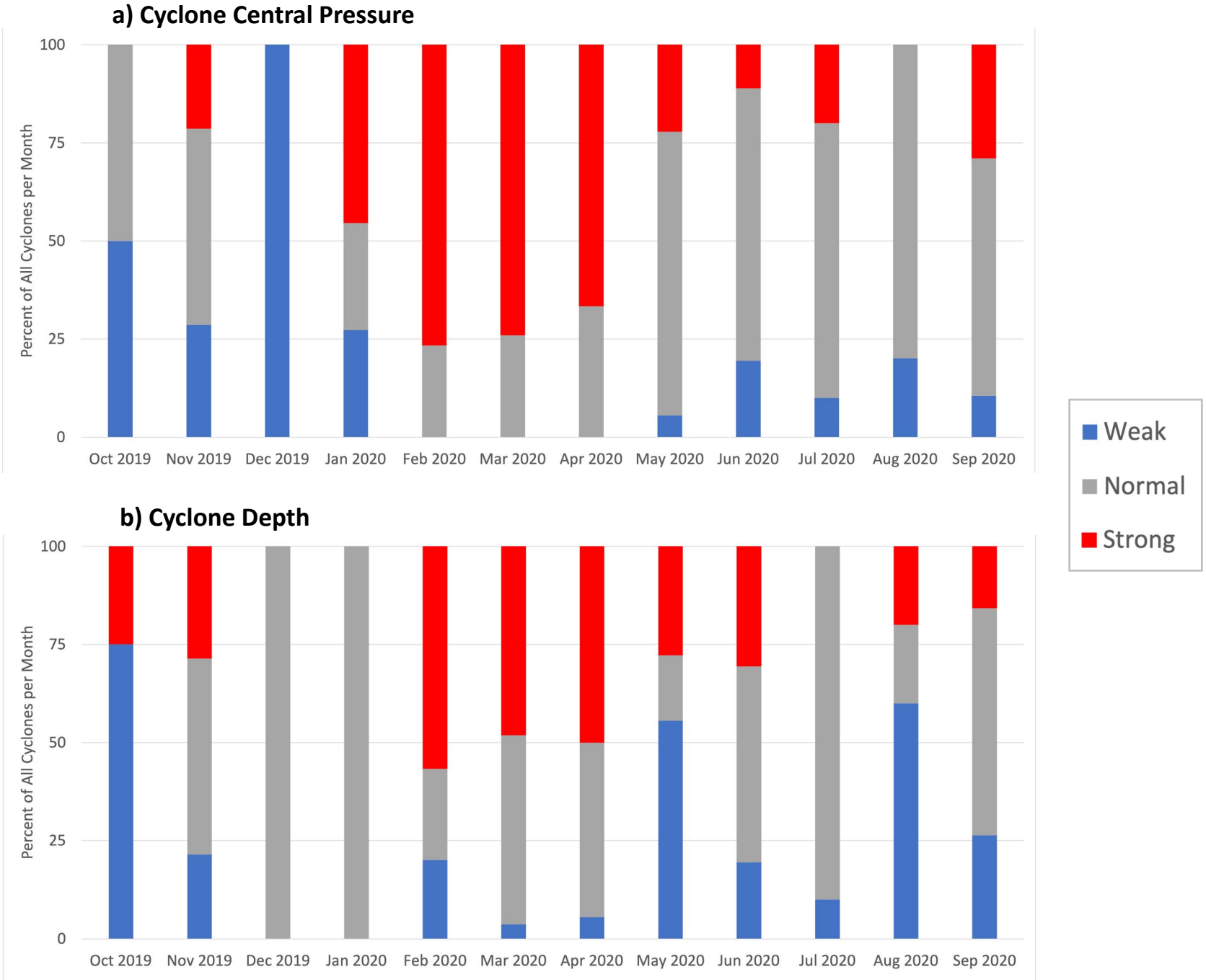
a) Cyclone Central Pressure
Percent of All Cyclones per Month
100
75
50
25
0
Oct 2019
Nov 2019
Dec 2019
Jan 2020
Feb 2020
Mar 2020
Apr 2020
May 2020
Jun 2020
Jul 2020
Aug 2020
Sep 2020
b) Cyclone Depth
Percent of All Cyclones per Month
100
75
50
25
0
Oct 2019
Nov 2019
Dec 2019
Jan 2020
Feb 2020
Mar 2020
Apr 2020
May 2020
Jun 2020
Jul 2020
Aug 2020
Sep 2020
Weak
Normal
Strong

Figure 8.

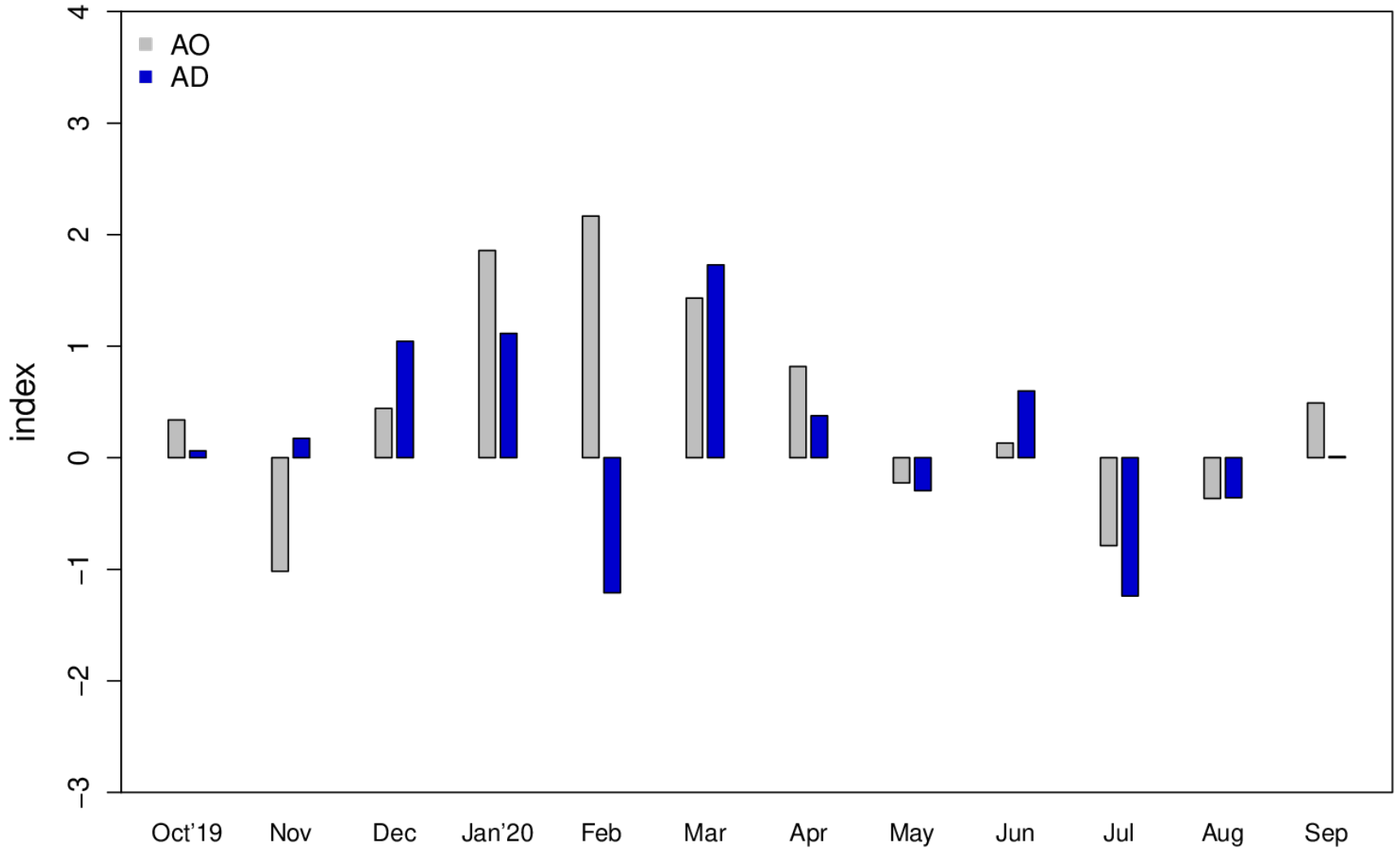
AO
AD
index
4
3
2
1
0
−1
−2
−3
Oct'19
Nov
Dec
Jan'20
Feb
Mar
Apr
May
Jun
Jul
Aug
Sep

Figure 9.

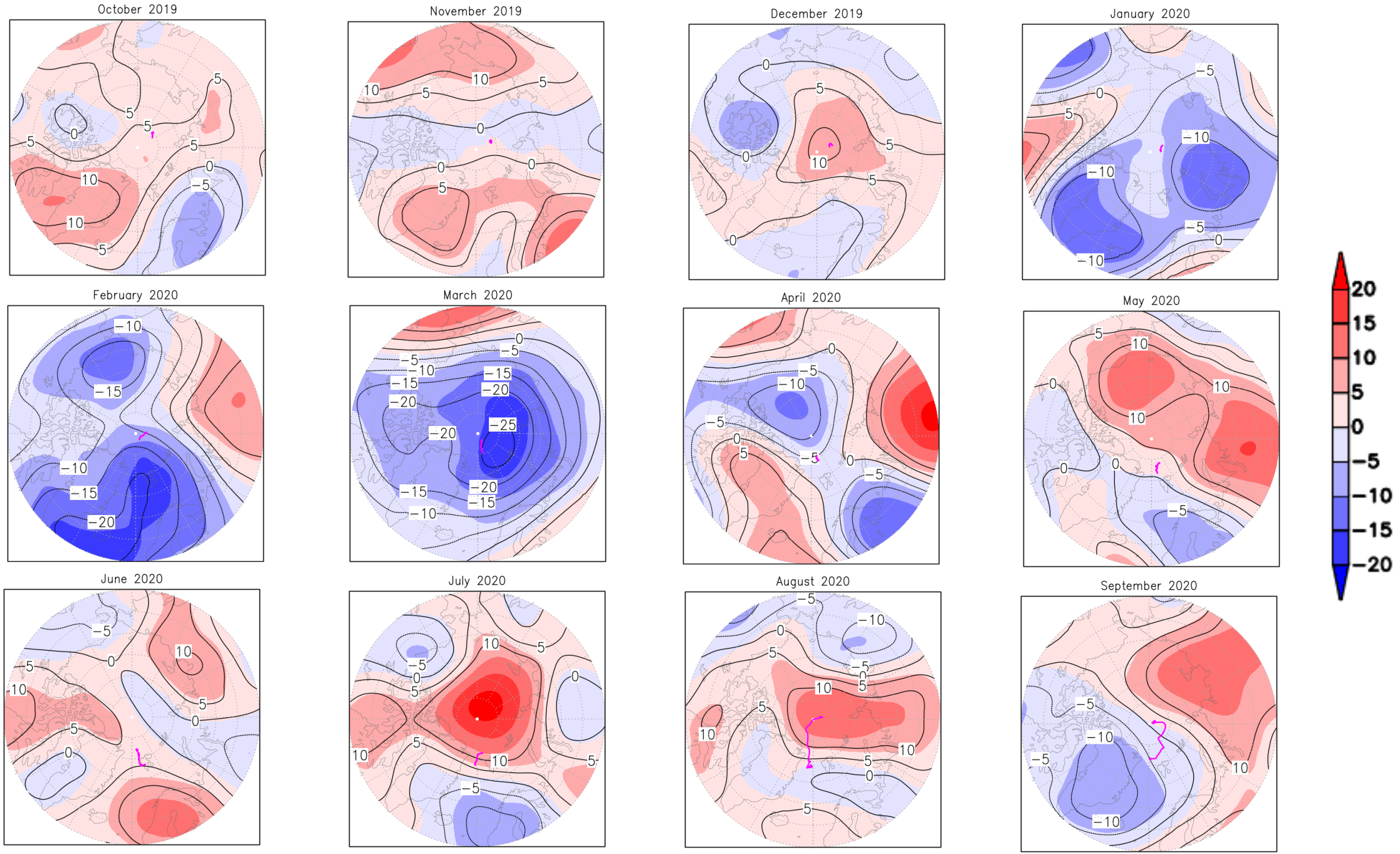
October 2019
November 2019
December 2019
January 2020
February 2020
March 2020
April 2020
May 2020
June 2020
July 2020
August 2020
September 2020
20
15
10
5
0
−5
−10
−15
−20

Figure 10.

Please find our response to all comments (in blue).

Editor:

Please increase axis labels of some of the figures (i.e. Figure 1, 4) and try to make font sizes reasonable consistent among the manuscript figures.
We have increased the axes labeling in the according figures.

Please reformat the Supplemental Materials document using the attached example as a format guide. Please include a cover page, add page numbers, and check for consistent font size of text and table and figure captions.
We have reformatted our supplementary material according to the example. We have consistent font size (12) for all text and captions, except that the font size of the table content is smaller (10), otherwise the table gets too wide and does not fit on an A4 page.

Please find our response to all comments (in blue).

Reviewer 1:

This is a well written paper and will be useful for those wanting to see "at a glance" the contextual / background meteorological conditions during the MOSAiC campaign.

We thank the reviewer for the time and effort they spent reading our manuscript and for the suggestions for improvement, which we considered. Please see below.

Usually meteorological data are compared against a 30-year climatology. In this case it would be 1981 - 2010, rather than the 1979 - 2020 data presented here. Indeed, the authors should avoid using their data in the "climatological" window. If the window of 1981 - 2010 is used, this could also be used as a mechanism by which the last 10 years could be analysed, as well as the year 2019-2020.

First, we stress that we did not include the MOSAiC year in the climatology 1979-2019; this is stated in the text of section 2: "This does not include the MOSAiC year and is so based on the period from 1 January 1979 to 30 September 2019."

Second, data from 1979-present are used for most Arctic climate studies and we are interested in seeing how the MOSAiC year compares to this widely used time period. Therefore, we have used this long-term period as the reference in our paper. But, we also understand your point. Therefore, we have calculated and plotted the timeseries using the 30-year climatology of 1981-2010. Exemplarily, we show you this for mean sea level pressure and near-surface air temperature in the below Figure R1. This is directly comparable to Figure 1a and Figure 1c of our paper. It does show that our presented results are robust with respect to the findings of 'anomalous' events and periods and that our conclusions do not depend on the chosen climatological reference period. We have included an according statement in section 2, which reads: "The application of a standard 30-year climatological reference period from 1981-2010 confirms our conclusions about the 'anomalous' events.".

Third, we have also considered your suggestion to look at the last 10 years. For this, we have calculated the statistics (median, IQR, 5th and 95th percentiles) also for the period 2010-2019, and have included the 5th and 95th percentiles in the Figures 1 and 2 as new (green) lines; see the updated Figures 1 and 2. We have used these results to interpret to what extent the MOSAiC year is anomalous under the 'new Arctic' conditions. We have included a new paragraph that discusses the addition of 2010-2019 statistics in section 3.1.1, which reads: "Arctic extremes have changed in the recent decade, e.g. expressed by a clear shift of the extreme minimum temperature (5th percentile) towards warmer temperatures and frequently higher maximum temperature (95th percentile) particularly during autumn-winter, compared to the long-term statistics (Figure 1). But, the classification of specific MOSAiC conditions as 'normal' or 'anomalous', as discussed below, still persists based on the recent 2010-2019 period (Figures 1 and 2)."

It is clear to see why temperature is used in the analyses, as well as the pressure and wind speed. However, the liquid water content is a different proposition, and it is not clear what utility the authors have used the data for. The LWC can determine the moisture profile within the atmosphere and are therefore useful for commenting on the vertical lapse rates (how temperature decreases with height).

Sorry, but we think you have misinterpreted what we present in the paper. We do not present cloud liquid water content (LWC), because that is less reliable in reanalysis than the other variables. Instead, we present the total column water vapor (TCWV), which is the vertically integrated water vapor. We considered TCWV because it is an indicator of anomalous moisture advection events and because of its impact on downwelling longwave radiation. Finally, we emphasize that we focus in our study on the near-surface meteorological conditions (see

abstract and introduction) and do not include the analysis of the vertical atmospheric structure. We agree with you that the latter is interesting too, but this is beyond this study and should be considered in future analyses of the MOSAiC year data.

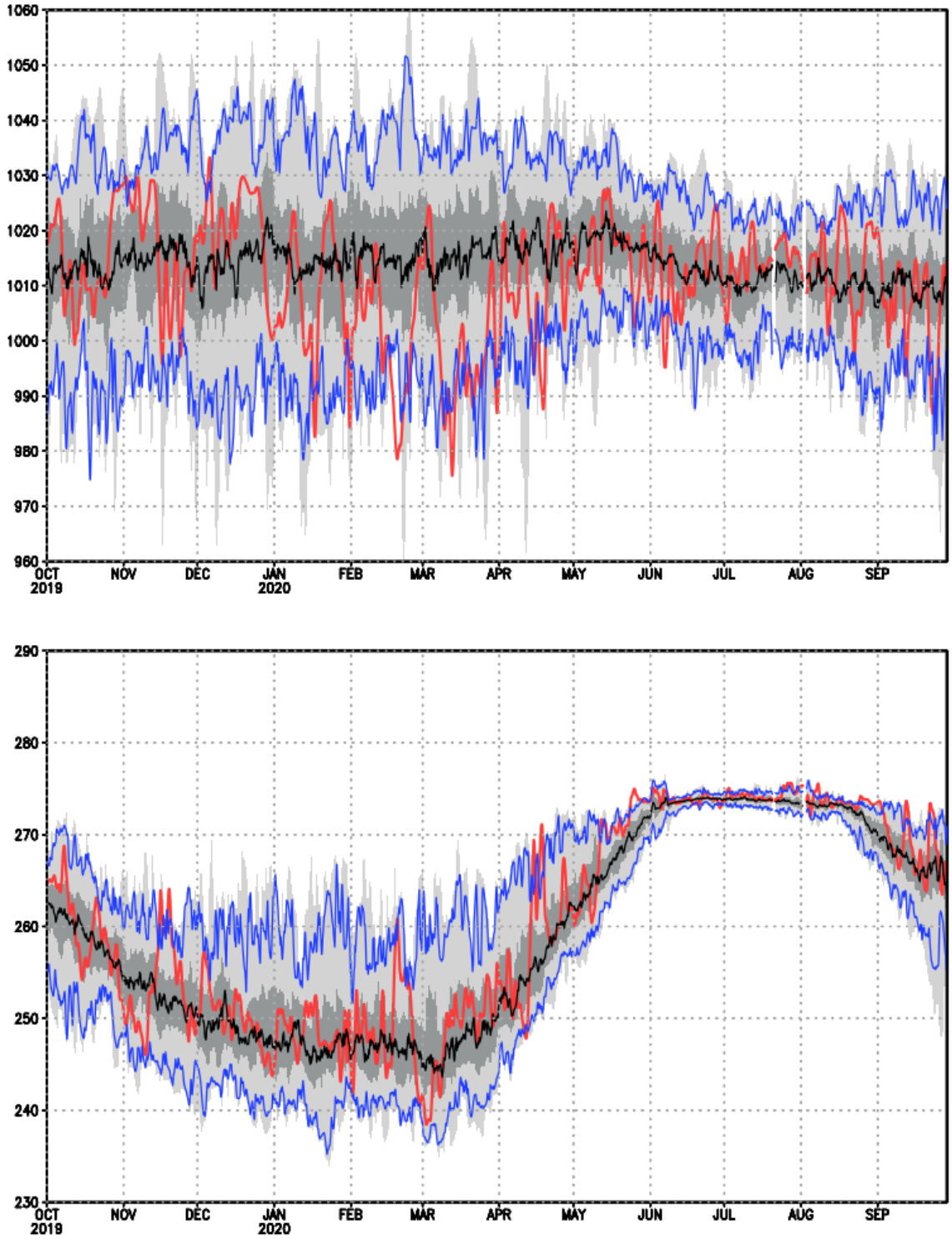

Figure R1: as Figs. 1a,c, but using 1981-2010 as the climatological reference period, top: mean sea level pressure, bottom: near-srfc. air temperature.

It might be worth looking at the different precipitation metrics in the ERA dataset, rather than relying on LWC.

Please see above, we do not analyze LWC. We do not include neither LWC nor clouds and precipitation as we know that they have high uncertainty in reanalyses. Thus, we chose to not include the 'condensate variables' in our analysis since these are less reliable than the other variables we have analyzed. It is worth noting that detailed observations of cloud and condensate were made as a part of MOSAiC, and future papers will certainly analyze these observations in detail.

Wind direction is always difficult to interpret in terms of long-term statistics, particularly as there is a sharp discontinuity around North (the 0, 360). It might be better to look at the vector wind (U,V) components.

According to your comment, we have removed the wind direction from Table 1 and have included instead both wind components u and v. Actually, we hardly discuss the wind direction in the paper; the only place we show this is Table 1. In our paper text we particularly discuss the anomalous northerly wind in March and April. As this is hard to interpret from the u and v components in the table, we have decided to calculate and include wind roses to display the wind direction. We show the wind roses for March and April in a new figure (new Figure 6; accordingly, we re-numbered the following figures) and for the other months of the year in the supplementary material in a new figure (new Figure S6; accordingly, we re-numbered the following supplemental figures). The according text and references are included in the text.

The work on the heat flux is useful - it might also be worth taking a look at the cloudy /clear statistics from the ERA5 dataset.

Please see also our related comments above to LWC and precipitation. We don't want to get into the 'condensate variables' in the reanalysis since these are less reliable than the other variables we have analyzed. We do not have much confidence in the ERA5 cloud cover so we do not want to include that in this paper. Since there were detailed cloud and radiation measurements made during MOSAiC, future papers will certainly look at how cloud cover impacts the surface energy budget.

The paper is descriptive, but it might be worth expanding on whether or not it was large scale forcing (far field advective) or locally driven radiative (balance of shortwave / longwave / latent / sensible) processes which dominated.

We appreciate this suggestion and would like to point out several instances in section 3.1.3 where we relate anomalous warm or cold conditions with specific forcing. Specifically, we highlight the following events in the manuscript, while detailed analysis of other anomalous conditions will need to await further analysis in future publications.

- Anomalous cold in early November was related to the negative phase of AO
- Anomalously warm conditions in mid-November was related to a storm event and moisture intrusion from the North Atlantic
- December warm event was associated with a moist intrusion
- Mid-February warm event was associated with a moist intrusion from Siberia
- Cold conditions in early March were associated with a regional cold anomaly centered over Fram Strait
- Anomalous spring warmth (April and May) along the MOSAiC drift track was consistent with anomalous warmrth across much of the Arctic
- Summer warmth was consistent with lower than normal sea ice concentration

The "jump" in the net radiation and surface energy budget (Figure 2c and d) in June 2020 needs closer inspection.

Sorry, but you have unfortunately missed that this feature in the time series is explained in the figure caption: “Note: The abrupt increase of net radiation (and thus SEB) at the beginning of June is associated with the parking of *Polarstern* in the ice-free fjord of Svalbard between MOSAiC leg3 and leg4.“

Please find our response to all comments (in blue).

Reviewer 2:

I think this will be an important paper cited by in most subsequent MOSAiC papers. I have a couple of small queries that should be easy to clear up.

We thank the reviewer for the time and effort they spent reading our manuscript and for the few suggestions for improvement, which we considered. Please see below.

It is not clear if observations from the Polarstern during the MOSAiC campaign are assimilated into ERA5. If they are, ERA5 for the MOSAiC year may not be representative of the rest of the ERA5 reanalysis as it will have extra observation in an area normally data sparse. I don't think this is an important criticism but I think it is worthy of mention if the observations are not included and discussion of the impact if they are.

Yes, ERA5 assimilates the Polarstern data that is distributed on the GTS and that is the soundings and the weather station data. We have included this information in Section 2.

Although this provides extra observations in the central Arctic for the specific MOSAiC year, also many other observations are regularly available in this area. This applies in particular buoy data and satellite data. And, data from previous expeditions such as Tara, N-ICE2015, ACLOUD/PASCAL were available in other years. Therefore, our hypothesis is that ERA5 for the MOSAiC year is representative of the rest of the reanalysis period.

A detailed assessment of the impact of additional MOSAiC measurements on the reanalysis is only possible if data denial experiments are performed with the forecast systems. This means, the reanalysis needs to be rerun without the MOSAiC data included in the assimilation system. Additional data likely improved the quality of ERA5 data. Nevertheless, it is speculation to estimate in which way this potentially alters the data compared to previous years, since it likely depends various variables such as the synoptic situation or the season.

A very minor point - I feel that section 3.1 is rather long and it would make the paper more reader friendly if the section were subdivided into different time periods - I think this would be quite easy.

We have included according sub-headings. Associated with this we have re-arranged a few paragraphs.

Meteorological conditions during the MOSAiC expedition: Normal or anomalous?

Annette Rinke[1)#], John Cassano[2, 3)#*], Elizabeth Cassano[2)], Ralf Jaiser[1)], Dörthe Handorf[1)]

[1)] Alfred Wegener Institute, Helmholtz Centre for Polar and Marie Research (AWI), Potsdam, Germany
[2)] National Snow and Ice Data Center, Cooperative Institute for Research in Environmental Sciences (CIRES), University of Colorado, Boulder, CO, USA
[3)] Department of Atmospheric and Oceanic Sciences, University of Colorado, Boulder, CO USA

[#] These authors contributed equally to this work.

[*] Corresponding author: John Cassano (john.cassano@Colorado.EDU)

Abstract. This paper sets the near-surface meteorological conditions during the Multidisciplinary drifting Observatory for the Study of Arctic Climate (MOSAiC) expedition in the context of the interannual variability and extremes within the past four decades. Hourly ERA5 reanalysis data for the *Polarstern* trajectory for 1979-2020 are analyzed. The conditions were relatively normal ~~considering~~ given that they were mostly within the interquartile range of the preceding four decades. Nevertheless, some anomalous and even record-breaking conditions did occur, particularly during synoptic events. Extreme cases of warm, moist air transported from the northern North Atlantic or northwestern Siberia into the Arctic were identified from late fall until early spring. D~~Then, d~~aily temperature and total column water vapor were classified as being among the top-ranking warmest/wettest days or even record-breaking based on the full record. Associated with this, the longwave radiative fluxes at the surface were extremely anomalous for these winter cases. The winter and spring period was characterized by more frequent storm events and median cyclone intensity ranking in the top 25th percentile of the full record. During summer, near melting point conditions were more than a month longer than usual and the July and August 2020 mean conditions were the all-time warmest and wettest. These record conditions near the *Polarstern* were embedded in large positive temperature and moisture anomalies over the whole central Arctic. In contrast, unusually cold conditions occurred during the beginning of November 2019 and in early March 2020, related to the Arctic Oscillation. In March, this was linked with anomalously strong and persistent northerly winds associated with frequent cyclone occurrence to the southeast of the *Polarstern*.

1. Introduction

The Multidisciplinary drifting Observatory for the Study of Arctic Climate (MOSAiC) expedition (Shupe et al., 2020) was a yearlong (October 2019-September 2020) drift with the sea ice across the central Arctic Ocean, based around the German icebreaker *Polarstern*. Its overarching goal was to study the climate of the "new" Arctic (https://mosaic-expedition.org/wp-content/uploads/2020/12/mosaic_scienceplan.pdf), which is characterized by warming temperatures, retreating and thinning sea ice, and changing atmospheric and ocean circulation (e.g., Stroeve and Notz, 2018; Box et al., 2019). A major goal of MOSAiC is to improve the understanding of Arctic climate processes and the complex interactions and feedbacks within the coupled atmosphere-ice-ocean-biogeochemistry-ecosystem. To place the single MOSAiC year of data in a broader climate context it is important to know if the expedition occurred under 'normal' or 'unusual' conditions. This study focusses on the near-surface meteorological conditions experienced during the MOSAiC expedition and compares these to a long-term reanalysis record.

Before the start of MOSAiC, the conditions in the Arctic were exceptional with record warm air temperatures in summer 2019, the longest ice-free summer period since 1979, and unusually thin sea ice (Krumpen et al., 2020). The MOSAiC winter of 2019/2020 attracted a lot of attention, because the Arctic stratosphere featured an exceptionally strong and cold polar vortex and related extreme ozone loss, accompanied by an unprecedentedly positive phase of the Arctic Oscillation (AO) during January-March 2020 (Wohltmann et al., 2020; Lawrence et al., 2020; Manney et al., 2020). Related to this, unprecedented warming over Eurasia and particularly the Kara and Laptev Seas regions was reported for those winter months. During spring and summer 2020 mean temperatures were above normal for most of the Arctic (Ballinger et al., 2020), with Siberia observing record-breaking temperatures associated with a persistent Siberian heatwave (Overland and Wang, 2020). For the actual MOSAiC drift path and speed, and the sea-ice conditions (such as thickness, melt ponds etc.), the atmospheric circulation patterns and associated anomalies in near-surface wind, temperature and radiation are relevant.

The aim of this paper is to characterize the 12-month time series of near-surface meteorological conditions during the MOSAiC expedition and compare this with the previous 41 years (1979-2019). This study is based on the European Centre for Medium-range Weather Forecasts (ECMWF) reanalysis ERA5 (Hersbach et al., 2020). This reanalysis has been selected because of its high resolution (ca. 30 km horizontal and 1 hourly temporal resolutions) and use of a significantly more advanced 4D-var assimilation scheme, as well as its improved performance over the Arctic (Graham et al., 2019a, b). Still, similar to other reanalyses, ERA5 struggles with a few Arctic specifics. These include a positive wintertime 2 m air temperature bias which is largest during very cold stable conditions and is associated with poorly represented surface inversions and turbulent heat fluxes over sea ice (Graham et al., 2019b). However, since these are systematic biases, and because this study compares ERA5 conditions during the MOSAiC year to ERA5 conditions during the previous four decades these biases are likely not relevant. Future work, based on MOSAiC meteorological observations can provide a comparison between ERA5 and the actual meteorology observed during the expedition, but since these data are currently still being quality controlled, the current reanalysis-only results presented here provides a first assessment of the MOSAiC expedition meteorology and its comparison to the prior decades.

By assessing the MOSAiC's meteorological conditions in the context of interannual variability and extremes within the past four decades, this study will document if the MOSAiC conditions, along the drift track, were close to the long-term mean or exceptional and identify any record conditions. Furthermore, this analysis will highlight some interesting meteorological situations and synoptic events that can be the focus of future studies.

2. Data based on ERA5

Statistics of near-surface meteorological conditions and cyclones, based on ERA5, are calculated for each month of the MOSAiC year, from October 2019 to September 2020, as well as for the previous 41 years from 1979 to 2019. The latter period is used as the long-term reference. The statistics for the MOSAiC and pre-MOSAiC years are compared. For the latter, the median, interquartile range (25^{th}-75^{th} percentiles, IQR), 5^{th} and 95^{th} percentiles, and minimum and maximum of the variables are calculated based on 1979-2019. This does not include the MOSAiC year and is so based on the period from 1 January 1979 to 30 September 2019. It is important to note that ERA5 assimilates the *Polarstern* sounding and the weather station data that is distributed on the GTS.

~~We cover the full annual cycle of MOSAiC. This includes the passive (drifting) and active (steaming) ship time. At the following dates the *Polarstern* was located at a permanent ice station and passively drifting with the ice: 4 October 2019 - 15 May 2020 (Legs 1-3), 18 June 2020 - 30 July 2020 (Leg 4), and 22 August 2020 - 19 September 2020 (Leg 5).~~

To characterize the MOSAiC data with respect to the previous four decades, we apply the following description. If the data are within the IQR we consider them being 'normal'. If the data are out of IQR but still within the 5^{th}-95^{th} percentile range we consider them 'unusual' or 'anomalous'. If data are above/below the 95^{th}/5^{th} percentiles we consider them being 'extremely anomalous' or 'record-breaking'. This is equivalent with the three top highest/lowest rankings considering the full record 1979-2020. The application of a standard 30--year climatological reference period from 1981-2010 confirms our conclusions about the 'anomalous' events. In addition, we used the recent decade 2010-2019 as a reference period to characterize the state of the 'new Arctic'.

We cover the full annual cycle of MOSAiC. This includes the passive (drifting) and active (steaming) ship time. At the following dates the *Polarstern* was located at a permanent ice station and passively drifting with the ice: 4 October 2019 - 15 May 2020 (Legs 1-3), 18 June 2020 - 30 July 2020 (Leg 4), and 22 August 2020 - 19 September 2020 (Leg 5).

2.1 Near-surface meteorological data

The following ERA5 data were used to characterize the near-surface meteorological conditions: mean sea level pressure (MSLP), 2 m and 850 hPa air temperature, 10 m wind speed and direction, total column water vapor (TCWV), and surface radiation components. For these variables, hourly ERA5 data from 1 October 2019 through 30 September 2020 (Figure S1) were extracted for the four grid points nearest the *Polarstern* position. Along the same MOSAiC trajectory the hourly four-grid-points data were extracted for the preceding 41 years of 1979-2019. In addition to the time series, box plots (with median, IQR, minimum-maximum range) and the Probability Density Functions (PDFs) from Kernel density estimation with Gaussian kernels are presented to identify changes in the distribution of the considered variables. To identify any record conditions, we ranked both the daily and monthly values for the full period from 1979-2020. All results are the same regardless if one simply averages the four grid points or calculates a distance-weighted average, thus the first approach is used. Spatial monthly anomaly maps with respect to the 41-year climatology are calculated to indicate regionally unusual conditions.

2.2 Cyclone detection and tracking

Along with the near-surface meteorological conditions described above, cyclones that impacted the MOSAiC drift were analyzed. For this analysis all cyclone centers whose closed isobars encompass the *Polarstern* location were considered. The cyclone tracking algorithm used for this work is based on an algorithm described in Serreze et al. (1993) and Serreze (1995) and updated by Crawford and Serreze (2016). The details of this algorithm can be found in Crawford

and Serreze (2016), but a brief description is provided here. The cyclone tracking algorithm was applied to 6-hourly ERA5 MSLP data, interpolated to a 50 km equal area scalable Earth (EASE) grid (Brodzik and Knowles, 2002), consistent with previous applications of this algorithm.

Gridded MSLP, excluding high elevation grid points (higher than 1500 m), are evaluated for minima by comparing each grid point with the surrounding 8 grid points. Each minimum found is then assigned a unique identifier. At the next time period, the MSLP minima are again located and compared with the MSLP minima from 6 hours prior. A given minimum is determined to be a continuation of a previous track if it meets the conditions of where the cyclone may have traveled based on an assumed maximum propagation speed and first guess of where the cyclone would be located 6 hours later. If there is no previous track associated with a minimum, it is defined as a cyclogenesis event and a new cyclone track identifier is created.

For each 6-hourly period the cyclone tracking algorithm identifies the latitude and longitude of all cyclone centers, their area based on the last closed isobar that surrounds the pressure minima, multiple intensity metrics and the unique track identifiers. For this work the MSLP at the center of the cyclone and its depth (defined as the difference between the central pressure and the pressure of the last closed isobar) are used to define each cyclone's intensity. The maximum ERA5 10 m wind speed within each cyclone's area is used as an additional intensity metric. Monthly cyclone statistics (median, IQR, minimum and maximum values) are calculated for the number of cyclone centers whose closed isobars encompass the *Polarstern*, cyclone central MSLP, cyclone depth, cyclone area maximum 10 m wind speed, and *Polarstern* MSLP and wind speed for each cyclone occurrence. These statistics for the MOSAiC year are compared with the same statistics for the 1979-2019 period.

It is possible that multiple minima of MSLP are present within the identified cyclone area. If this is the case, the cyclone is referred to as a multi-center cyclone and each minimum is tracked, although they will all have the same cyclone area, defined by the last closed isobar that encircles the minima. For this work, each MSLP minima that is part of a multi-center cyclone is treated as a separate cyclone event and will have unique latitude, longitude central pressure and depth, but will have the same cyclone area maximum wind speed and *Polarstern* MSLP and wind speed.

Statistics for each cyclone track impacting the MOSAiC drift were recorded and are described in Section 3.2 and listed in the supplementary material (Tables S1 to S12, Figure S2) to serve as a reference for future synoptic studies.

2.3 Indices for large-scale atmospheric circulation

To provide a broader context for the near-surface conditions that occurred during the MOSAiC expedition, the large-scale atmospheric circulation, based on geopotential heights at 250 hPa and 500 hPa (Z250, Z500) as well as monthly teleconnection indices are included in this study. Here, we consider the key teleconnections for the Arctic region, namely the Arctic Oscillation (AO) pattern and the Arctic Dipole (AD) pattern. We derived these patterns and their respective indices from an Empirical Orthogonal Function (EOF) analysis of monthly MSLP anomaly in the three-month period centered on the considered month over 50-90°N. This domain is larger than that used in most studies analyzing the AD pattern in winter (e.g., Wu et al., 2006) or summer (e.g., Cai et al., 2018), but ensures that the domain boundaries do not induce an artificial preference of certain pattern structures (see, e.g. the discussion in Legates, 2003 and Overland and Wang, 2010). In all months, the AO pattern has been identified as the first EOF, whereas the AD pattern occurred as the second, third or fourth EOF pattern. The latter underlines that the AD pattern is less stable than the AO, nonetheless, several studies have shown its critical importance for the Arctic circulation and sea-ice decline (e.g., Wu et al., 2006; Cai et al., 2018; Watanabe et al., 2006; Zhang, 2015). The corresponding AO and AD spatial

patterns are shown in Figure S3 exemplarily for the mid-month of each season, i.e. January, April, July and October. The base period for the pattern calculation is 1979-2020 to account for recent changes in the structure and amplitude of the teleconnection patterns.

3. Results

3.1 Near-surface meteorological conditions

3.1.1 Anomalous conditions over the annual cycle

Overall, the full time series of the near-surface meteorological variables (Figure 1) and surface radiative fluxes (Figure 2) indicate that the conditions during MOSAiC were mostly within the recorded minimum-maximum range of the preceding 41 years. This applies also for the frequently occurring storms and moisture intrusion events, which show their clear signatures in the timeseries of MSLP, wind, temperature, TCWV and radiation. However, the figures also highlight that there were frequently conditions over short periods associated with synoptic-scale events that emerge as unusual by being outside of the IQR or were record-breaking. To put that in a monthly context, Table 1 highlights those specific months and variables when two-thirds of the hourly data were outside of the IQR, which we classify as being 'particularly' anomalous monthly conditions. Table 1 shows that for most variables and most months between one third and two thirds of the hourly data during MOSAiC were within the IQR, and here we consider this to be 'normal'. If more than two-thirds of the hourly data during MOSAiC were within the IQR we define this as being 'particularly' normal and note that only a few variables / months show these conditions. Furthermore, a ranking of the monthly and daily mean data of all years 1979-2020 (Figure 3) identifies the several record conditions along the MOSAiC track position.

To put the anomalous conditions during MOSAiC as a whole in the context of interannual variability, i.e. to estimate how many periods of particularly anomalous conditions are normal per year, we calculated the occurrence of 'outside IQR' conditions for past nine years (2010-2019, Table S13). If we compare the occurrence of particularly anomalous conditions during MOSAiC (Table 1) with the average over the past nine years (synonymously for the 'recent new Arctic'), it becomes clear that the MOSAiC year was unusual with respect to emerged anomalous TCWV and air temperature. For those more than twice as ~~much~~many conditions outside of the IQR over the year occurred compared to the average conditions.
In order to evaluate changes in Arctic extremes in the recent past the 5th and 95th percentiles for surface meteorological conditions (Figure 1) and surface radiative fluxes and energy budget (Figure 2) have been calculated for the decade 2010-2019. Comparison of these recent decade percentiles to those calculated for the 1979-2019 period reveal a clear shift of the extreme minimum temperature (5th percentile) towards warmer temperatures and frequently higher maximum temperature (95th percentile) particularly during autumn-winter, compared to the long-term statistics (Figure 1). But, the classification of specific MOSAiC conditions as 'normal' or 'anomalous', as discussed below, still persists based on the recent 2010-2019 period (Figures 1 and 2).

3.1.2 Anomalous low pressure in winter-spring

The MSLP during the MOSAiC winter and early spring (January to April 2020) was often in the lowest quartile of MSLP values of the previous four decades (Figures 1 and 4). In the monthly context, the MOSAiC median MSLP for those months is shifted towards smaller MSLP compared to the long-term median. In February-April, the MOSAiC median MSLP was lower than the 25th percentile from the climatology (Figure 4), and the largest shift by ca. 20 hPa occurred in March. Furthermore, in February and March, more than 70% of the hourly MSLP data were outside of the IQR (below the 25th percentile; Table 1), which we define as

'particularly' anomalous. During February-March 2020, the MSLP was extremely anomalously low during almost the entirewhole month (Figure 1), associated with frequent cyclone occurrence (section 3.2) and an extreme positive AO phase (section 3.3). The monthly mean MSLP in the central Arctic showed an anomaly of more than -15 hPa (Figure 5) and was along the MOSAiC track record-breaking, namely the top/3rd lowest pressure for February/March months in the climatology (Figure 3). Similarly, the April 2020 monthly MSLP anomaly was as low as -15 hPa over the central Arctic (Figure 5). The monthly mean MSLP along the track was anomalously low with the 5th lowest pressure (Figure 3), associated with the impact of a moisture intrusion event (discussed in the next sectionthe next paragraph).

3.1.3 Anomalous warm/moist and cold/dry conditions

Autumn-Winter

October 2019, the first month of MOSAiC, started with normal monthly mean near-surface meteorological conditions (Table 1, Figure 3), but this occurred as conditions varied from anomalously positive T2M, MSLP, TCWV, LWD at the beginning of the month, followed by negative and then again positive anomalies compared to the previous decades (Figures 1 and 2). However, in all months from October 2019 to January 2020, the coldest temperatures shifted towards warmer temperatures, i.e. extreme cold temperatures did not occur as in the past (Figure 4). In December and January, the IQR was reduced compared to previous decades. Temperatures from ca. -25°C to -20°C (248 K to 253 K) occurred more frequently, but extreme warm temperatures above -15°C (258 K) were absent, compared to the previous 4four decades.

The normal mean November conditions (Figure 3, Table 1) come due to canceling effects of two anomalous cold and warm periods. The first ten days in November 2019 were anomalously cold (Figure 1) and ranked among the coldest seven, compared to the climatology; Nov.10 was even the 3rd coldest of the daily climatology (Figures 1 and 3). The relative cold temperatures are related to the negative phase of the AO in November 2019 (section 3.3). The anomalously warm conditions in mid-November were triggered by a strong storm event consisting of two cyclones passing over the MOSAiC track during ca. Nov. 16-20 (Figures 1 and S2, Table S2) associated with a prominent moisture intrusion transporting warm, moist air from the northern North Atlantic into the Arctic. This brought extreme warm temperature anomalies of ca. 15 K, such that the temperature was not only outside of the IQR but also higher than the 95th percentile. These days were classified as being among the six warmest of the climatological record; Nov. 18-19 were the 3rd warmest and Nov. 20 was the 2nd warmest in the climatology for those days. The associated moist anomalies of ca. 5 kg/m^2 (Figure 1) were also extremely anomalous with TCWV above the 95th percentile. The TCWV of those days were classified as being among the seven highest values in the climatology. Nov. 19-20 had record-breaking TCWV, Nov. 21 the 2nd highest and Nov. 16 the 3rd highest (Figure 3). Associated with these warm, moist conditions, the longwave radiative fluxes at the surface were also extremely anomalous. The downward longwave radiation during that event was among the seven highest in the climatology. For downward longwave radiation, Nov. 19-20 had the 2nd highest and Nov. 16 the 3rd highest values of the daily climatology, and the net longwave radiation indicates the extremely low radiation loss into space (Figures 2 and 3).
The dominating event for the anomalous warming in December was also associated with an intrusion of warm, moist air that occurred at the beginning of December (Dec 3-5, 2019; Figure 1), but this event was not associated with a cyclone directly impacting the MOSAiC drift track. This was a shorter-lived event that originated from northwestern Siberia. The temperature at MOSAiC was anomalous, at the edge of the 95th percentile, and ranked as the 5th warmest period in the climatology. The TCWV during this event was extremely anomalous. Dec. 3 and 5 ranked as the 4th highest, while Dec.4 had the 2nd highest TCWV in the daily climatology (Figure 3).

The longwave and net radiation (Figure 2) was similarly extremely anomalous as for the November event.
The third anomalous winter warming event occurred in mid-February (Feb. 18-22, 2020; Figure 1) again triggered by an intrusion of warm, moist air from northwestern Siberia into the Arctic. This caused similar anomalous temperature, TCWV and radiation as described above. As with the other two, this event is clearly identified as an event with hourly/daily extremely anomalous temperature, TCWV and longwave radiation, based on the ERA5 climatology. The near record-breaking days were Feb.19-20, classified as the 5th-4th for temperature and as the 3rd-4th for TCWV (Figure 3). Importantly, the mean February above-normal temperatures at the near surface (Figure 5) and at 850 hPa height (Figures S4 and S5) covers the whole Eastern Arctic region and were influenced by the record-breaking positive AO phase (section 3.3).

Spring

~~Following this anomalous warmth,~~E~~ e~~arly March was characterized by unusually cold conditions (Figures 1 and S4) outside of the prior decades' IQR. The near-surface air temperature of the first five days were among the five coldest of the record (Figure 3), while the 850 hPa temperature, including the following five days, were among the 10 coldest. Accordingly, the TCWV was in the first days of March anomalously low (Figure 1) with record low values during March 4-5 showing the second lowest value of the climatological record for those days. Starting in mid-March the temperature mostly remained within the IQR, indicating relatively normal conditions for this time of year (Table 1). In the monthly mean, March 2020 was characterized by slightly below-normal temperatures at the near surface (Figure 5) and at 850 hPa height (Figure S5). This was embedded in a regional cold anomaly with the center over the Fram Strait region, which was linked with anomalous northerly winds (Figure 6) bringing cold polar air into that region (Figure 5) and also led to the rapid southward drift of the MOSAiC floe. (Note: Wind roses for all months are shown in Figure S6). This was associated with the strong negative MSLP anomaly over the Arctic Ocean (Figure 5; see section 3.1.2~~below~~) related with the positive AO phase (section 3.3) and frequent cyclone occurrence to the south and east of the MOSAiC drift track (section 3.2).
~~The MSLP during the MOSAiC winter and early spring (January to April 2020) was often in the lowest quartile of MSLP values of the previous four decades (Figures 1 and 4). In the monthly context, the MOSAiC median MSLP for those months is shifted towards smaller MSLP compared to the long-term median. In February-April, the MOSAiC median MSLP was lower than the 25th percentile from the climatology (Figure 4), and the largest shift by ca. 20 hPa occurred in March. Furthermore, in February and March, more than 70% of the hourly MSLP data were outside of the IQR (below the 25th percentile; Table 1), which we define as 'particularly' anomalous. During February-March 2020, the MSLP was extremely anomalously low during almost the whole month (Figure 1), associated with frequent cyclone occurrence (section 3.2) and an extreme positive AO phase (section 3.3). The monthly mean MSLP in the central Arctic showed an anomaly of more than -15 hPa (Figure 5) and was along the MOSAiC track record-breaking, namely the top/3rd lowest pressure for February/March months in the climatology (Figure 3). Similarly, the April 2020 monthly MSLP anomaly was as low as -15 hPa over the central Arctic (Figure 5). The monthly mean MSLP along the track was anomalously low with the 5th lowest pressure (Figure 3), associated with the impact of a moisture intrusion event (discussed in the next paragraph)~~
In spring, the MOSAiC expedition experienced a few other records. Above-normal monthly mean temperatures occurred over the whole Arctic Ocean in April and May 2020 with a maximum warm anomaly over northwestern Siberia (Figures 5 and S5). The all-time warmest May temperature in the 1979-2020 ERA5 record was noted in May 2020 (Figure 4).

The monthly mean MOSAiC-trajectory temperature of April 2020 was not unusual, but ranked among the warmest 12 Aprils in the climatology due to southerly warm air advection bringing extreme warm temperatures that occurred during April 15-21, 2020 (Figure 1). This warming was preceded by a brief cold period, with temperatures in the lowest quartile of the record associated with northerly winds (Figure 6). The associated temperature jump was extreme (ca. +20 K) such that the temperature during the specific warm days was record-breaking compared to~~onsidering~~ the climatology (Figures 1 and 3). The temperature on April 16 and 19 was the highest ever and on April 18 and 20 it was the 2nd highest for those days' records. The event was associated with record-breaking moisture (April 16, 19-20 had all-time highest TCWV for those days) and longwave radiation (April 19 had the 2nd lowest and April 20 had the lowest ever net longwave radiation loss on these dates) (Figures 1-3).

In May 2020 the monthly mean MOSAiC temperature was among the six warmest in the full record (Figure 3), which was caused by the anomalous warm temperatures in the second half of May when daily record-breaking temperatures occurred during days 17, 25-29 (Figures 1, 3, 4, and S4). The temperature distribution for this month clearly shows a significant shift of the median (out of the IQR) and, as stated above, had the all-time warmest May temperature (Figures 4 and S4). Associated with the anomalous warm conditions, the monthly mean TCWV was the all-time highest for May over the past four decades (Figure 3). This is consistent with a changed TCWV distribution, which is shifted towards a higher median (out of the IQR) and is flatter and broader (indicated by the significantly larger IQR box) (Figure 4). Table 1 supports the classification as particularly anomalous conditions as more than two-thirds of the hourly temperature and TCWV data in May 2020 were outside of the IQR. A cyclone event that occurred around mid-May (Figure S2, Table S8) caused record-breaking conditions during those days (Figure 3) that resulted in daily temperatures that were among the 3rd highest in the ERA5 climatology. May 17 showed the highest ever recorded temperature for that day. In addition, the moisture was extremely anomalously high, e.g. the TCWV on May 14-15 ranked as the 3rd highest of the climatological record.

Summer

During summer, 2 m air temperatures near the melting point of ice persisted from late May until early September during MOSAiC. This period of near melting point conditions was more than a month longer than the 1979-2019 median (Figure 1) and is consistent with lower than normal sea-ice concentration along the MOSAiC drift track during the summer (Krumpen et al., 2021). The MOSAiC temperatures in July and August 2020 were especially anomalous (Table 1, Figures 1, 4, and S4) and the warmest of the 1979-2020 period (Figure 3). This is also clearly shown by the shift of the temperature distribution to warmer temperatures with the MOSAiC year's median temperature higher than the long-term 75th percentile (Figures 4 and S4). These record warm conditions near the *Polarstern* were embedded in large positive air temperature anomalies (up to 8 K) over the whole central Arctic (Figure S5). Furthermore, associated with the extreme warm conditions, the whole MOSAiC summer was moister than the climatological mean with daily TCWV anomalies of up to ca. 30 kg/m^2 (Figure 1). The TCWV distributions are significantly shifted towards higher median values for all summer months of June-September 2020, compared to the long-term median (Figure 4). The most anomalous conditions occurred in July-August, when both the median and the 25th percentile exceed the long-term 75th percentile. Along the MOSAiC track, both July and August 2020 show all-time highest monthly TCWV (Figure 3) with 73 and 88% of the hourly TCWV values in these months lying outside of the IQR (Table 1). Further, the all-time highest monthly hourly TCWV in the ERA5 record from 1979-2020 was observed in both June and August (Figure 4). In addition, positive monthly anomalies of ca. 4 kg/m^2 with respect to the climatology occurred over the whole central Arctic region (Figure 5). Finally, two distinct warm air mass intrusion events stand out

in middle of September, associated with rapid moisture and temperature increase (above the melting point) and record-breaking values (Figure 1). This implied a temporary positive surface energy budget, i.e. hours of melt conditions of the snow-ice surface (Figure 2).
The anomalous summer (May-September) conditions can be related to~~with~~ the changing sea ice. In earlier years, MOSAiC would have been deep in the ice pack, while in recent years the sea-ice extent is great~~strong~~ly reduced (e.g., Stroeve and Notz, 2018). Accordingly, MOSAiC was closer to the sea-ice edge (e.g., with a distance less than 200 km at the beginning of July; Krumpen et al., 2021) than earlier in the climatology, which is generally linked with warmer and wetter conditions.
~~To put the anomalous conditions during MOSAiC as a whole in the context of interannual variability, i.e. to estimate how many periods of particularly anomalous conditions are normal per year, we calculated the occurrence of 'outside IQR' conditions for past nine years (2010-2019, Table S13). If we compare the occurrence of particularly anomalous conditions during MOSAiC (Table 1) with the average over the past nine years (synonymously for the 'recent new Arctic'), it becomes clear that the MOSAiC year was unusual with respect to emerged anomalous TCWV and air temperature. For those more than twice as much conditions outside of IQR over the year occurred compared to the average conditions.~~

3.2 Cyclone activity

Many of the anomalous meteorological conditions discussed in the previous section were associated with cyclone events impacting the MOSAiC drift. The number of cyclone centers, based on 6-hourly data, whose closed isobars included the *Polarstern* drift from October 2019 to September 2020 are compared to the median, IQR and minimum and maximum range of monthly cyclones for the 1979 to 2019 period (Figure 7~~6~~a). Cyclone counts were below the long-term monthly median counts from October 2019 through January 2020, with less than 12 6-hourly cyclone occurrences impacting the MOSAiC drift in each of these four months. Cyclone counts were near or above the 75th percentile in February and March 2020, consistent with the persistently low pressure observed during these months (Figures 1, 4 and 5). Cyclone counts were near the long-term median in April, with counts well above the long-term median in May and June 2020. Low cyclone numbers were again observed in July and August, with counts near or below the 25th percentile in these months. This is in accordance with the positive MSLP anomaly over the central Arctic, which was as high as +10 hPa in July and +5 hPa in August (Figure 5). The MOSAiC year ended with very high cyclone counts in September 2020. Cyclone intensity, as characterized by cyclone central MSLP and depth, as well as MSLP at the *Polarstern*, highlight the anomalous conditions during late winter and early spring 2020, with less unusual conditions for the remainder of the MOSAiC year (Figures 7~~6~~b, 7~~6~~c, and S6). MOSAiC year cyclone central MSLP was above the long-term 75th percentile in October and near the long-term median in November 2019. MOSAiC year cyclone central MSLP was then below the long-term median from January to April 2020, with the MOSAiC year median being below the long-term 25th percentile from February to April 2020 (Figure 7~~6~~b), indicating much stronger than normal cyclones during these months. MOSAiC year cyclone central MSLP was near the long-term median from May through August with lower values (stronger cyclones) observed in September. The median monthly MOSAiC year cyclone depth and maximum cyclone wind speed (Figures 7~~6~~c and 7~~6~~d) are consistent with the monthly variability in cyclone central MSLP discussed above. These three metrics of cyclone intensity indicate that late winter into spring of the MOSAiC year experienced anomalously strong cyclones relative to the prior 40 years. This is consistent with the shift to a record positive AO during winter 2020 (section 3.3). The pressure and wind speed observed at the *Polarstern* during cyclone events (Figure S7~~6~~) were mostly consistent with the cyclone intensities discussed above, except for the ship

cyclone wind speed during March, which was below the long-term median, despite the monthly median wind speed being above the long-term 75th percentile (Figure 4).
For each 6-hourly cyclone occurrence the percentile ranking of each cyclone intensity metric was calculated compared to the 1979-2020 ERA5 data. Cyclone occurrences were classified as strong if the cyclone depth was in the top 25th percentile, normal if the depth was between the 25th and 75th percentiles (i.e. within the IQR), and weak if the depth was in the lowest 25th percentile for each month in the 1979-2020 period. The opposite thresholds were used for cyclone central MSLP to identify strong, normal or weak cyclones. More than 50% of cyclones that impacted the *Polarstern* from February to April 2020 were classified as strong based on their central pressure (Figure 8~~7~~a), consistent with the low MSLP seen in Figure 1 and the distribution of cyclone MSLP shown in Figure 7~~6~~b. Ranking the cyclones by depth revealed a similar pattern of an unusually large number of strong cyclones during these late winter and early spring months (Figure 8~~7~~b). The remainder of the MOSAiC year was characterized by near normal to below normal frequency of strong cyclones and near normal to above normal occurrence of normal or weak cyclones.
Based on the cyclone track information from the Crawford and Serreze (2016) cyclone tracking algorithm, all tracks whose cyclone areas encompassed the MOSAiC drift in each month were identified. For each of these tracks the start and end date and time and location of the track and the start and end date and time of when the cyclone area included the Polarstern were recorded. In addition, the minimum central MSLP, minimum *Polarstern* MSLP, maximum depth, maximum cyclone area 10 m wind speed and maximum *Polarstern* 10 m wind speed when the cyclone area encompassed the *Polarstern* were recorded (Tables S1-S12) to serve as a reference for future synoptic studies. The track locations, for each month of the MOSAiC expedition, are shown in Figure S2.
The anomalous warm and moist events discussed in section 3.1 (Figure 1) can be linked to specific cyclones impacting the MOSAiC drift track. The shift from anomalously warm to cold conditions in mid-November was associated with a cyclone that started in North America on 11 Nov. 2019 and traversed the central Arctic towards Siberia (Figure S2) and whose maximum intensities were in the strongest 25th percentile of all November cyclones since 1979 (Table S2). The shift from anomalously warm to cold conditions in late February was associated with a cyclone track that started on 18 Feb. near Novaya Zemlya (Figure S2) whose maximum intensity was near the strongest 10th percentile (Table S5). The exceptionally low MSLP in March 2020 was associated with 11 separate cyclone tracks from 11 to 25 March impacting the *Polarstern* (Figure S2). These cyclones' central MSLP ranked in the top 25th percentile of all March storms from 1979-2019 (Table S6). The location of these cyclones, to the south and east of the *Polarstern*, resulted in persistent northerly winds during mid-March (Figure 6), which caused a rapid southward drift of the *Polarstern* (Krumpen et al., 2021). The warm and moist conditions occurring in mid to late April 2020 were associated with three cyclone tracks impacting the *Polarstern* from 16 to 19 April whose intensities ranked in or near the top 25th percentile, in terms of wind speed at the *Polarstern* and central MSLP (Figure S2, Table S7).

3.3 Large-scale atmospheric circulation

Overall, the monthly time series of the Arctic Oscillation (AO) and Arctic Dipole (AD) teleconnection indices (Figure 9~~8~~) indicate an unusual course from late autumn 2019 until early spring 2020. A strong negative AO phase in November was followed by a near neutral AO in December. The most striking circulation anomaly of the MOSAiC year develops during winter. The MOSAiC winter (January-March 2020) was characterized by an exceptionally strong and cold polar vortex with Z500 and Z250 anomalies as large as -25 gpm (Figure 10~~9~~). This was accompanied by a record-breaking positive phase of the AO (Figure 9~~8~~) and related near-surface warm anomalies over northern Eurasia (which was unprecedented in the MERRA-2

record back to 1980; Lawrence et al., 2020) and cold anomalies in Alaska, northern Canada and Greenland (Figures 5 and S5). Due to its location, MOSAiC was mainly affected by the AO accompanied warming in February (Figures 5 and S5) and accordingly showed above-normal temperatures (Figures 1 and S4; section 3.1). In addition, the center of the Z500 and Z250 circulation anomalies changed its position during winter (Figure 10~~9~~) due to the impact of the prevailing phase of the AD pattern, which was negative in February, and positive in January and March. The exceptional large-scale flow configuration in February with strong positive AO and strong negative AD is related with the very high cyclone occurrences in that month (Figure 7~~6~~). Another key feature related to this anomalous atmospheric circulation in winter was the associated anomalous wind, which was experienced by MOSAiC (section 3.1). The wind speed was particularly anomalously high (Figure 4) and the wind direction was particularly anomalous (northerly) in March (Figure 6, Table 1), which pushed the drift more quickly across the transpolar drift.

During the remaining months of the MOSAiC expedition, the large-scale atmospheric conditions were quite normal with not many unusual index values. Only in July a rather strong quasi-barotropic anticyclonic anomaly develops over the Arctic Ocean with positive MSLP anomalies as large as +10 hPa (Figure 5) and Z500 anomalies as large as +20 gpm (Figure 10~~9~~). These circulation anomalies correspond to the strong negative phase of both the AO and the AD teleconnection patterns.

4. Conclusions

Overall, the MOSAiC expedition represents a changing Arctic with higher temperature and more moisture in particular during summer and more intense winter-spring storms. This relates with the changed background state, often called the 'New Arctic': Compared to earlier years, the *Polarstern* has seen thinner sea ice in winter and lower sea-ice concentration in summer (Krumpen et al., 2021). The main findings for the meteorological conditions along the yearlong MOSAiC track based on ERA5 reanalysis data and compared to the past four decades are:

- For most variables and months, the MOSAiC conditions were fairly typical: The hourly and daily near-surface meteorological variables and surface radiative fluxes during MOSAiC were mostly within the recorded IQR of the preceding four decades. For most variables and months up to two-thirds of the hourly MOSAiC data were inside of this IQR. Most of the MOSAiC year's monthly median values were also within the IQR. Unusual were the significantly higher wind speed in March, the lower MSLP in February-April, and the higher temperature and TCWV in May-August, with the all-time hourly record high temperature in May and TCWV in June and August.
- The conditions at MOSAiC were impacted by a series of interesting extreme events, such as extreme storm (exceptional strong wind speed and low pressure) and moisture intrusion (exceptional high total column water vapor) events. Those show a clear signature in the temperature and moisture data, which were classified not only as unusual (by being out of the IQR), but as extremely anomalous (by being larger than the 95th percentile) or even record-breaking considering the long-term statistics. The most noteworthy events, associated with extreme warm and moist conditions, occurred from late fall until early spring in mid-November, the beginning of December, mid-February, mid-April, and mid-May. In winter, these events were associated with extremely anomalous downward and net longwave radiation at the surface.
- The number of cyclones and their intensity were anomalous during the MOSAiC winter and spring, with monthly cyclone counts well above the long-term median from February through June 2020. The cyclones in the period from late winter to spring (February to April 2020) were also stronger than normal with more than 50% of cyclone events classified as being strong.

- A list of all cyclone events that impacted the MOSAiC drift is provided and could be further analyzed in follow-up process-oriented studies. Of interest to analyze is for example the coupling between free-troposphere, boundary-layer, and surface processes, and sea-ice impacts during cyclone events (e.g., Persson et al., 2020).
- During summer, the near melting point conditions were more than a month longer than usual (compared to the 1979-2019 median) in accordance with the all-time warmest and wettest mean July and August conditions. These summer record warm and moist conditions occurred not only near the *Polarstern* but over the whole central Arctic.
- Not many record low temperature appeared during MOSAiC, but unusually cold conditions occurred during the beginning of November and early March (linked with extremely anomalous low MSLP), associated with the large-scale atmospheric circulation conditions (AO phase).

References

Ballinger, TJ, Overland, JW, Wang, M, Bhatt, US, Hanna, E, Hanssen-Bauer, I, Kim, SJ, Thoman, RL, Walsh, JE. 2020. Arctic Surface Air Temperature. *Arctic Report Card*. DOI: http://dx.doi.org/10.25923/gcw8-2z06

Box, J, 19 coauthors. 2019. Key indicators of Arctic climate change: 1971-2017. *Environmental Research Letters* 14: 045010. DOI: http://dx.doi.org/10.1088/1748-9326/aafc1b

Brodzik, MJ, Knowles, KW. 2002. EASE-Grid: A Versatile Set of Equal-Area Projections and Grids. Chapter 5 in Michael F.Goodchild (Ed.) *Discrete Global Grids: A Web Book*. Santa Barbara, California USA, National Center for Geographic Information & Analysis. https://escholarship.org/uc/item/9492q6sm.

Cai, L, Alexeev, VA, Walsh, JE, Bhatt, US. 2018. Patterns, impacts, and future projections of summer variability in the Arctic from CMIP5 models. *Journal of Climate* 31: 9815-9833. DOI: http://dx.doi.org/10.1175/JCLI-D-18-0119.1

Crawford, AD, Serreze, MC. 2016. Does the summer Arctic frontal zone influence Arctic Ocean cyclone activity? *Journal of Climate* 29: 4977-4993.

Graham, RM, Hudson, SR, Maturilli, M. 2019a. Improved performance of ERA5 in Arctic gateway relative to four global atmospheric reanalyses. *Geophysical Research Letters* 46: 6138-6147. DOI: http://dx.doi.org/10.1029/2019GL082781

Graham, R, Cohen, L, Ritzhaupt, N, Segger, B, Graversen, R, Rinke, A, Walden, VP, Granskog, MA, Hudson, SR. 2019b. Evaluation of six atmospheric reanalyses over Arctic sea ice from winter to early summer. *Journal of Climate* 32: 4121-4143. DOI: http://dx.doi.org/10.1175/JCLI-D-18-0643.1

Hersbach, H, 42 coauthors. 2020. The ERA5 global reanalysis. *Quarterly Journal of the Royal Meteorological Society* 146(730): 1999-2049. DOI: http://dx.doi.org/10.1002/qj.3803

Krumpen, T, 37 coauthors. 2020. The MOSAiC ice floe: sediment-laden survivor from the Siberian shelf. *The Cryosphere* 14: 2173-2187. DOI: http://dx.doi.org/10.5194/tc-2020-64

Krumpen, T, 15 coauthors. 2021. The MOSAiC Drift: Along-track ice conditions from space and comparison with previous years. submitted to *The Cryosphere*

Lawrence, ZD, Perlwitz, J, Butler, AH, Manney, GL, Newman, PA, Lee, SH, Nash, ER. 2020. The remarkably strong Arctic stratospheric polar vortex of winter 2020: Links to record-breaking Arctic Oscillation and ozone loss. *Journal of Geophysical Research Atmosphere* 125: e2020JD033271. DOI: http://dx.doi.org/10.1029/2020JD033271

Legates, DR. 1993). The effect of domain shapes on principal components analysis: a reply. *International Journal of Climatology* 13: 219-228. DOI: http://dx.doi.org/10.1002/joc.3370130207

Manney, GL, Livesey, NJ, Santee, ML, Froidevaux, L, Lambert, A, Lawrence, ZD, Millán, LF, Neu, JL, Read, WG, Schwartz, MJ, Fuller, RA. 2020. Record- low Arctic stratospheric ozone in 2020: MLS observations of chemical processes and comparisons with previous extreme winters. *Geophysical Research Letters*, 47: e2020GL089063. DOI: http://dx.doi.org/10.1029/2020GL089063

Overland, JE, Wang, M. 2010. Large-scale atmospheric circulation changes are associated with the recent loss of Arctic sea ice. *Tellus A* 62: 1-9. DOI: http://dx.doi.org/10.1111/j.1600-0870.2009.00421.x

Overland, JE, Wang, M. 2020. The 2020 Siberian heat wave. *International Journal of Climatology* 41 (Suppl. 1): E2341-E2346. DOI: http://dx.doi.org/10.1002/joc.6850

Persson, OPG, Shupe, M, deBoer, G, Perovich, D, Haapala, J, Graeser, J, Solomon, A, Cox, C, Hutchings, J. 2020. Structure of Arctic cyclones during MOSAiC and their surface impacts, AGU Fall Meeting, December 1-17.

Serreze, MC. 1995. Climatological aspects of cyclone development and decay in the Arctic. *Atmosphere and Ocean* 33: 1-23, DOI: http://dx.doi.org/10.1080/70559900.1995.9649522

Serreze, MC, Box, JE, Barry, RG, Walsh, JE. 1993. Characteristics of Arctic synoptic activity 1952-1989. *Meteorology and Atmospheric Physics* 51: 147-164. DOI: http://dx.doi.org/10.1007/BF01030491

Shupe, MD, Rex, M, Dethloff, K, Damm, E, Fong, AA, Gradinger, R, Heuzé, C, Loose, B, Makarov, A, Maslowski, W, Nicolaus, M, Perovich, D, Rabe, B, Rinke, A, Sokolov, V, Sommerfeld, A. 2020. The MOSAiC Expedition: A Year Drifting with the Arctic Sea Ice, *Arctic Report Card*, DOI: http://dx.doi.org/10.25923/9g3v-xh92

Stroeve, J, Notz, D. 2018. Changing state of Arctic sea ice across all seasons. *Environmental Research Letters* 13: 103001, DOI: http://dx.doi.org/10.1088/1748-9326/aade56

Watanabe, E, Wang, J, Sumi, A, Hasumi, H. 2006. Arctic dipole anomaly and its contribution to sea ice export from the Arctic Ocean in the 20th century. *Geophysical Research Letters* 33: L23703, DOI: http://dx.doi.org/10.1029/2006GL028112

Wohltmann, I, von der Gathen, P, Lehmann, R, Maturilli, M, Deckelmann, H, Manney, GL, et al. 2020. Near- complete local reduction of Arctic stratospheric ozone by severe chemical loss in spring 2020. *Geophysical Research Letters* 47: e2020GL089547. DOI: http://dx.doi.org/10.1029/2020GL089547

Wu, B, Wang, J, Walsh, JE. 2006. Dipole Anomaly in the winter Arctic atmosphere and its association with Arctic sea ice motion. *Journal of Climate* 19: 210-225, DOI: http://dx.doi.org/10.1175/JCLI3619.1

Zhang, R. 2015. Mechanisms for low-frequency variability of summer Arctic sea ice extent. *Proceedings National Academy of Science USA* 112: 4570-4575, DOI: http://dx.doi.org/10.1073/pnas.1422296112

Funding information. AR and DH acknowledge funding by the Deutsche Forschungsgemeinschaft (DFG, German Research Foundation) - project 268020496 TRR 172, within the Transregional Collaborative Research Center "ArctiC Amplification: Climate Relevant Atmospheric and SurfaCe Processes, and Feedback Mechanisms (AC)3. AR, DH, RJ acknowledge funding by the German Federal Ministry of Education and Research (BMBF) via the project "Synoptic events during MOSAiC and their Forecast Reliability in the Troposphere-Stratosphere System (SynopSys)" with grant 03F0872A. JC and EC acknowledge funding from the United States National Science Foundation grants PLR 1603384 and OPP 1805569.

Acknowledgments. We greatly thank Julius Eberhard and Ida Sigusch for their help with data preparation and graphics that provided the basis for the time series analysis. We thank Matthew Shupe for useful comments that strengthened the paper. We thank ECMWF and DKRZ for providing ERA5 reanalysis data, generated using Copernicus Climate Change Service Information (C3S). This manuscript was produced as part of MOSAiC with the tag MOSAiC20192020 and the Project_ID AWI_PS122_00.

Contributions. Conception, design and initial manuscript draft: AR, JC; Analysis of data: AR, JC, EC, DH; Interpreting data, drafting and revising the article: all authors; Final approve of the version to be submitted: all authors

Competing of interest. The authors have declared that no competing interests exist.

Code/data availability. The position of *Polarstern* is made available by AWI at the dashboard website https://dashboard.awi.de/data-xxl/rest/data?sensors=vessel:polarstern:hydrins_1:latitude&sensors=vessel:polarstern:hydrins_1:longitude&beginDate=2019-09-20T18:00:00&aggregate=minute&limit=10000&streamit=true&withQualityFlags=false&withLogicalCode=false&format=text/csv.
ERA5 data are made available by the Copernicus Climate Change Service (C3S) at https://cds.climate.copernicus.eu/cdsapp#!/home. Copernicus Climate Change Service (C3S) (2017): ERA5. Fifth generation of ECMWF atmospheric reanalyses of the global climate. Copernicus Climate Change Service Climate Data Store (CDS), 2017–2020.

Table 1. Percent of time (%) that each variable was outside of the 1979-2019 interquartile range (IQR) (first row for each variable) and the percent of time (%) being below/above the 25th/75th percentile (second row for each variable) for each month of the MOSAiC trajectory, based on hourly ERA5 data. Variables: MSLP - mean sea level pressure, TCWV - total column water vapor, T2M - 2m air temperature, T850 - 850hPa air temperature, US10 - 10m wind speed, ~~UD10 - 10m wind direction,~~ U10 and V10 - 10m zonal and meridional wind components, LWD - longwave downward radiation at the surface, SWD - shortwave downward radiation at the surface, NetRad - net radiation at the surface. Note that the occurrence of SWD is limited during polar night conditions (Oct.-Mar.). Any month with more than 2/3 (66%) of the MOSAiC hourly data of a variable outside of the IQR is highlighted in bold to indicate particularly anomalous conditions. Any month with more than 2/3 of the MOSAiC hourly data of a variable inside of the IQR (i.e. 34% out of IQR) is highlighted in italic and underlined for labeling it as being particularly normal.

	2019			2020								
	Oct.	Nov.	Dec.	Jan.	Feb.	Mar.	Apr.	May	June	July	Aug.	Sep.
MSLP	40 13/27	60 19/41	48 6/42	51 46/5	**73** 73/0	**74** 72/2	65 58/7	38 34/4	45 25/20	*31* 7/24	47 13/34	37 27/10
TCWV	50 12/38	46 17/29	47 1/46	39 5/34	64 24/40	56 28/28	54 20/34	**69** 14/55	57 6/51	**73** 1/72	**88** 1/87	58 17/41
T2m	38 16/22	61 32/29	*26* 7/19	*27* 9/18	48 16/32	*30* 21/9	45 10/35	**73** 10/63	64 20/44	56 4/52	**68** 8/60	47 8/39
T850	52 6/46	60 33/27	54 0/54	*12* 1/11	37 8/29	60 45/15	59 24/35	**69** 15/54	49 8/41	**75** 8/67	**85** 0/85	35 2/33
US10	37 26/11	48 18/30	58 41/17	52 32/20	50 11/39	**67** 19/48	52 16/36	50 17/33	52 22/30	52 26/26	50 32/18	55 30/25
~~UD10~~	~~56~~ ~~37/19~~	~~57~~ ~~36/21~~	~~**69**~~ ~~24/45~~	~~57~~ ~~30/27~~	~~38~~ ~~28/10~~	~~**76**~~ ~~32/44~~	~~64~~ ~~19/45~~	~~41~~ ~~34/7~~	~~56~~ ~~23/33~~	~~**81**~~ ~~58/23~~	~~35~~ ~~24/11~~	~~49~~ ~~25/24~~
LWD	51 22/28	57 28/29	*33* 6/27	38 9/29	61 27/34	38 15/23	58 23/35	65 12/53	63 9/54	**69** 8/61	**84** 2/82	51 15/36
U10	43 32/11	52 35/17	53 13/40	59 41/18	61 50/11	57 11/46	56 12/44	**67** 52/15	42 16/26	**67** 60/7	*30* 25/5	53 30/23
V10	41 30/11	64 43/21	50 33/17	42 23/19	50 20/30	**68** 60/8	61 37/24	55 21/34	61 36/25	44 38/6	59 15/44	47 14/33
SWD	-	-	-	-	-	48 16/32	60 28/32	50 34/16	55 44/11	45 31/14	**79** 71/8	58 51/7
NetRad	57 23/34	55 23/32	40 6/34	46 10/36	65 34/31	52 15/37	62 25/37	50 29/21	50 23/27	46 19/27	**71** 18/53	56 23/33

Figures titles and legends

Figure 1: Comparison between MOSAiC and climatological near-surface meteorological conditions. The comparison presents time series of a) mean sea level pressure (hPa), b) 10m wind speed (m/s), c) 2m air temperature (K), and d) total column water vapor (kg/m^2) at *Polarstern* position and based on ERA5 (average over the four nearest grid points). Red line: MOSAiC year, black line: median over 1979-2019, dark grey shading: interquartile range, blue lines: 5th and 95th percentiles, light grey shading: min-max range from 1979-2019 data. The 5th and 95th percentiles from the recent 2010-2019 period are shown with green lines and indicate the full range of this period's data. Based on hourly data, 24 hour running means are plotted. Note: The abrupt decrease of the wind speed and changes in the range of variability of temperature at the beginning of June is associated with the parking of *Polarstern* in the ice-free fjord of Svalbard between MOSAiC leg 3 and leg 4 and the associated sheltering.

Figure 2: Comparison between MOSAiC and climatological surface energy fluxes. The comparison presents time series of surface fluxes (W/m^2) of a) downward shortwave radiation, b) downward longwave radiation, c) net radiation, and d) surface energy budget (SEB) at *Polarstern* position and based on ERA5 (average over the four nearest grid points). Red line: MOSAiC year, black line: median over 1979-2019, dark grey shading: interquartile range, blue lines: 5th and 95th percentiles, light grey shading: min-max range from 1979-2019 data. The 5th and 95th percentiles from the recent 2010-2019 period are shown with green lines and indicate the full range of this period's data. Based on hourly data, 24 hour running means are plotted. Note: The abrupt increase of net radiation (and thus SEB) at the beginning of June is associated with the parking of *Polarstern* in the ice-free fjord of Svalbard between MOSAiC leg3 and leg4. The abrupt decrease of SEB at the end of September is associated with temporarily reduction of sea-ice concentration near the ice edge in the Fram Strait and large upward turbulent heat fluxes.

Figure 3: Ranking of near-surface meteorological parameters during MOSAiC in context of the past four decades. The ranking is presented for monthly and daily mean data based on the full record of 1979-2020 for a) mean sea level pressure, b) 2m air temperature, c) total column water vapor, and d) surface net radiation at *Polarstern* position and based on ERA5 (weighted average over the four nearest grid points). Darkest red/blue: MOSAiC year had the highest/lowest value out of the past years data. The timestamp (start of the month) is given along the drift position.

Figure 4: Monthly comparison of near-surface meteorological conditions between MOSAiC and climatology. The comparison shows monthly median (red line), 25th and 75th percentile (box) and minimum and maximum (whiskers) of mean sea level pressure (hPa), 10m wind speed (m/s), 2m air temperature (K), total column water vapor (kg/m^2), and surface net radiation (W/m^2) for the MOSAiC year (right box and whisker plots) and for ERA5 1979 to 2019 (left box and whisker plot).

Figure 5: Spatial anomalies of monthly near-surface meteorological conditions during MOSAiC. Monthly anomaly of 2m air temperature (color shading; K), mean sea level pressure (black isolines; hPa), and total column water vapor (green isolines; kg/m^2; only plotted for anomalies $\geq \pm 2$ kg/m^2) for the MOSAiC year, compared to the previous four decades. The MOSAiC drift trajectory in the specific month is included as mangenta line.

Figure 6: Comparison of wind direction between MOSAiC and climatology for spring. The wind direction distribution shown as wind roses for March and April. Red filled: MOSAiC year, black encircled: 1979-2019. Based on hourly data. The other months of the year are shown in the Supplemental Material (Figure S6).

Figure 7~~6~~: Monthly cyclone statistics comparison between MOSAiC and climatology. The cyclone statistics shows (a) Monthly count of 6-hourly cyclone occurrence for the MOSAiC year of October 2019 to September 2020 (red asterisks) and median (red line) with 25th and 75th percentile (box) and minimum and maximum (whiskers) for ERA5 from 1979-2019. (b-d) Monthly median (red line), 25th and 75th percentile (box) and minimum and maximum (whiskers) of (b) cyclone central pressure, (c) cyclone depth and (d) maximum cyclone 10 m wind speed for the MOSAiC year (right box and whisker plots) and for ERA5 1979 to 2019 (left box and whisker plots).

Figure 8~~7~~: Characteristics of cyclone strength during MOSAiC. Frequency of occurrence (%) of weak (blue), normal (grey), and strong (red) cyclones based on a) cyclone central pressure and b) cyclone depth during each month of the MOSAiC year from October 2019 to September 2020. Cyclone intensity is defined as weak if the central mean sea level pressure MSLP (depth) is in the top (bottom) 25th percentile, normal if the central MSLP (depth) is within the IQR and strong if the central MSLP (depth) is in the bottom (top) 25th percentile.

Figure 9~~8~~: Teleconnection indices for the MOSAiC year. Monthly indices of Arctic Oscillation (AO) and Arctic Dipole (AD) for October 2019 to September 2020. Based on ERA5 data. The corresponding spatial patterns are shown in Figure S3.

Figure 10~~9~~: Monthly anomalies of atmospheric circulation during MOSAiC. The circulation anomalies are presented by monthly anomaly of 500 hPa geopotential height (color shading; gpm) and 250 hPa geopotential height (isolines; gpm) for the MOSAiC year, compared to the previous four decades. The MOSAiC drift trajectory in the specific month is included as mangenta line.